HSE
Health & Safety Executive

Load factor calibration for ISO 13819 Regional Annex: Component resistance

Prepared by
MSL Engineering Limited
for the Health and Safety Executive

OFFSHORE TECHNOLOGY REPORT
2000/072

HSE
Health & Safety Executive

Load factor calibration for ISO 13819 Regional Annex: Component resistance

MSL Engineering Limited
MSL House
5-7 High Street
Sunninghill
Ascot
SL5 9NQ

HSE BOOKS

First published 2001

ISBN 0 7176 1975 3

FOREWORD

This document summarises a study undertaken by MSL Engineering Limited for the Health and Safety Executive to establish component resistance statistics (means and biases) pertaining to API RP2A (WSD and LRFD versions) and ISO 13819-2. The components considered are: tubular members, tubular joints, grouted pile-to-sleeve connections and foundation piles.

The purpose of the study was to provide input to a wider initiative leading to the calibration of environmental load factors for use in the NW European Regional Annex to ISO 13819-2.

CONTENTS

1. INTRODUCTION

Much industry effort has been expended in developing a new standard for offshore structures under the auspices of the International Standards Organisation (ISO). One part, ISO 13819-2[(1.1)], concerning fixed steel structures, is nearing completion. This document allows for regional variations arising from climatic and regulatory concerns by the instrument of regional annexes. The regional annexes, for example, could contain guidance on the load factors that should be used for designing structures in those regions.

In March 1999 the Health and Safety Executive (HSE) hosted a meeting of interested parties to discuss the way forward in the calibration of environmental load factors for use in the NW European Regional Annex to ISO 13819-2. As a result of the meeting, and following further discussions, MSL Engineering was commissioned to undertake a review of the resistance formulations in the ISO code in comparison with those in API RP2A LRFD[(1.2)] and API RP2A WSD[(1.3)]. The specific objectives of the work, reported herein, were to:

- identify and document the effects of the most significant changes (from API to ISO) to the resistance formulations, and

- determine the bias and COV associated with the various formulations.

Four components were specified for this study: tubular members, tubular joints, grouted pile-to-sleeve connections and foundation piles (capacity in soil). These components are addressed, respectively, in Chapters 2 to 5 of this report. Findings and conclusions from the study are summarised in Chapter 6.

2. TUBULAR MEMBERS

2.1 Code Provisions

The API WSD, API LRFD and ISO provisions for checking the adequacy of tubular members are similar in that all three codes give formulations for loads acting alone and loads acting in combination.

Tables 2.1(a) to (c) summarise and compare the provisions of the three codes. It can be seen that many of the provisions are at least equivalent across all three codes. For instance the ISO and API LRFD formulations for axial tension, bending and hydrostatic pressure are identical. The most significant differences lie with axial compression, particularly with respect to local buckling, and with some of the load interaction equations.

The overall column buckling formulae in API WSD reflects AISC provisions and differs from LRFD and ISO. The LRFD and ISO use a similar form of equation but use different coefficients. A lower capacity is given by ISO (compared to LRFD), the aim of which was to achieve a degree of harmony with European buckling curves.

The local buckling strengths in WSD and LRFD are given by the same equations and, when expressed as a proportion of the yield stress, are a function of geometry only. In ISO, local buckling strength is more properly recognised as being a function of material properties as well as geometry. The effect of material properties on local buckling is explored in Section 2.2.

The interaction equations for tension or compression with bending in ISO more closely follow API WSD than the LRFD versions. That is the ISO interactions are linear combinations, whereas LRFD uses a cosine interaction form.

The background to the development of the ISO provisions is fully described in Reference 2.1.

2.2 Comparison of Codes

The main differences between API WSD, API LRFD and ISO are illustrated in this section.

- Overall Column Buckling

  Figure 2.1 shows the characteristic column strength (ie. partial factors of safety set to unity), normalised with respect to the tubular yield stress, for ISO and API LRFD. The normalised strength is plotted against the non-dimensional column slenderness parameter λ as defined in the corresponding code (see Table 2.1(a)). In general λ is related to the critical stress that the tubular cross section can sustain without local buckling occurring. For columns comprising of thick (compact) cross sections, this critical stress is simply the yield stress and in this instance the calculated λ from ISO is equal to that of API LRFD. Thus the points representing the calculated ISO and API LRFD strengths fall on the same vertical line. On the other hand, a thin-walled tubular subject to local buckling will be assigned different λ values by the two codes because of their different formulations for local buckling. Therefore the plotted points become displaced, see Figure 2.1.

  A more useful comparison can be obtained when a consistent slenderness parameter is used for plotting data. In Figure 2.2, the ISO slenderness value has been chosen for this purpose (the API λ was used in calculating the API column strength of course).

Regarding this figure, a number of observations can be made. For thick-walled tubulars (D/t < 60), the strength of very stocky columns approach full yield, even at the characteristic level, because of the onset of strain hardening. At large slenderness, the API curve follows the Euler buckling curve (= $1/\lambda 2$) whereas the ISO curve stays at 10% below it. This 10% is the greatest difference across the entire slenderness range. Somewhat greater differences can be observed for the thin-walled (D/t = 120) tubulars. (It will be seen later that the comparisons of thin-walled tubular strength is also a function of the material yield stress. For Figures 2.1 to 2.3, a yield strength of 270mpa has been used.) The difference between API LRFD and ISO is greatest when the thin-walled column is short (ie. of low λ).

API WSD column strengths cannot be compared at a characteristic level because of the working stress format. However, the total (unfactored) load capacities can be compared as shown in Figure 2.3. Here the API LRFD and WSD loads are compared to ISO loads, with all resistance and load partial factors included in the calculation. The load capacities are dependent on the assumed environmental to gravity load ratio and a range of 2 to 4 has been explored. However, because the partial load factors for API LRFD and ISO are the same, the LRFD curves are the same in the three diagrams shown. As noted above the thick-walled LRFD curve starts at unity and steadily climbs to 1.11 (= 1/0.9) and demonstrates that LRFD will give more capacity than ISO. The LRFD thin-walled curve crosses the unity line; the short columns ISO gives greater capacity than LRFD but less at higher slendernesses. The API WSD curves consistently lie above both ISO and LRFD and particularly so for higher live/dead load ratios.

- Local Buckling

As noted in Section 2.1 and in the above discussion, there is a significant difference in the provisions of API and ISO for local buckling. In ISO, the fact that material properties as well as geometry influence the propensity for local buckling has been recognised. Figure 2.4 compares the ISO and API (LRFD or WSD, they are both the same in this respect) local buckling strengths. The upper diagram in this figure compares the local buckling strengths, normalised with respect to yield stress, as a function of the tubular slenderness (D/t). It is seen that the API provision results in a single curve which is independent of the yield stress. The ISO provision generates a family of curves related to yield as shown. Apart from a relatively small region around D/t = 60 and for higher strength steels, API gives lower local buckling strengths. The lower diagram of Figure 2.4 shows the ratio of API local buckling strength to that of ISO. The ratio will apply to very stocky (short) columns but for increasingly long columns, overall buckling may precipitate first and the role of local buckling is then diminished. This can be observed in the coalescence of the thick and thin walled buckling curves in Figure 2.2 and is also reflected in Figure 2.3.

- Hydrostatic Pressure

As noted in Section 2.1, the ISO and API LRFD provisions for hydrostatic pressure are identical. However, those in API WSD are somewhat different. Although the elastic hoop buckling stress (Fhe) is the same in all three codes, the derived critical hoop stress (Fhc) is calculated differently in WSD, see Table 2.1(b). The effect is illustrated in Figure 2.5. Because the pressure that can be sustained is directly proportional to Fhc, tubulars are nominally stronger according to ISO or API LRFD over the range where the elastic buckling stress lies between 0.55 and 6.2 times the yield stress. When partial load and resistance factors are considered, LRFD and ISO become closer to WSD. The WSD safety factor is 1.5 and the ISO/LRFD load and resistance factors are 1.3 and 1.25 respectively. These lead to an overall factor of 1.5/(1.3 x 1.25) = 0.92 on the ISO/LRFD capacity relative to WSD.

- Combined Loads

  ISO has tended to revert to the simpler interaction equations of API WSD rather than use the interaction equations of API LRFD. As an example, consider combined axial tension and bending, see Figure 2.6. The WSD and ISO interactions are linear in nature whereas API LRFD uses a cosine interaction.

2.3 Statistics

The database used in the development of the ISO provisions for tubular members was made available to this project by the Chairman of the relevant Technical Core Group. Checks were made against MSL in-house data and generally the ISO and MSL databases matched although the ISO database had more data for members under bending. The statistics given in the ISO commentary were largely confirmed although there were a few discrepancies. These relate to the increased bending data mentioned above and that the quoted ISO statistics have been derived from ISO Draft C (rather than Draft D) in some instances.

The ISO database actually consists of a number of individual databases, each containing test data to explore a particular aspect of behaviour (eg. local buckling under compression) or specimens subjected to the same type of loading. In recognition of future reliability studies, a single bias and COV covering all tubular members is perhaps more useful than a set of statistics for different load patterns. The individual databases (apart from the combined tension and pressure database) were amalgamated into one large database. All data were then analysed, for each code, by the equations given in the section for combined axial compression, bending and hydrostatic pressure. Specimens subjected to a single load type were therefore treated as having a combined load set with vanishingly small values of other load components. This approach has the advantage of reducing the propensity for error that may be associated with coding up a number of separate databases. It also reflects the practical situation where rarely is a member subjected to a single load system in reality. Naturally, the combined interaction equations tend to default to the unidirectional equations for single load components. For API WSD, the factors of safety, which are used in the combined interaction equations though not in the unidirectional equations, were chosen to ensure that such defaulting occurred (the axial compression safety factor is given as a range in the code rather than a specific value).

The statistics for all three codes are presented in Table 2.2. For ISO and API LRFD, statistics are provided for the case when the partial resistance factors are set to unity (note these statistics are nominally the ones quoted in the ISO commentary).

The derivation of the statistics was complicated by two aspects. Firstly, in ISO and API LRFD, different partial resistance factors are cited for different actions (compression, tension, bending and hydrostatic pressure). Secondly, many of the equations are non-linear in nature. Both of these aspects were resolved by inserting a modelling bias coefficient into the equations (and applied to each load component) and then adjusting the coefficient iteratively, for each specimen in turn, such that the interaction equation was exactly satisfied. The statistics were then derived from the set of modelling bias coefficients. This approach was also adopted by the ISO Technical Core Group for Members in deriving the ISO formulations.

Inspection of Table 2.2 reveals that, overall, ISO and API LRFD achieve very similar levels of reliability, both with a mean bias of 1.28 and a COV of about 12%.

Table 2.1(a)
Tubular Members Code Provisions

API WSD*			API LRFD			ISO		
Stress/ Parameter	Formulation	Limits	Stress/ Parameter	Formulation	Limits	Stress/ Parameter	Formulation	Limits
	AXIAL TENSION			AXIAL TENSION			AXIAL TENSION	
F_t =	$0.6F_y$		f_t	$f_t <= \phi_t F_{tn}$ (ϕ_t =0.95)		f_t	$f_t <= F_y/\gamma_{Rt}$ (γ_{Rt} = 1.05)	
	AXIAL COMPRESSION			AXIAL COMPRESSION			AXIAL COMPRESSION	
			f_c	$f_c <= \phi_c F_{cn}$ (ϕ_c =0.85)		f_c	$f_c <= F_c/\gamma_{Rc}$ (γ_{Rc} = 1.18)	
	Column Buckling			Column Buckling			Column Buckling	
F_a =	$\frac{(1-(Kl/r)^2/2C_c^2)F_y}{5/3+3(Kl/r)/(8C_c)-(Kl/r)^3/(8C_c^3)}$	Kl/r<Cc	F_{cn} =	$(1-0.25\lambda^2)F_y$	$\lambda<2^{0.5}$	F_c =	$(1-0.28\lambda^2)F_{yc}$	$\lambda<1.34$
				F_y/λ^2	$\lambda>2^{0.5}$	F_c =	$0.9F_{yc}/\lambda^2$	$\lambda>1.34$
F_a =	$12\pi^2E/(23(KL/r))$	Kl/r>Cc		$\lambda = Kl/\pi r\ (F_y/E)^{.5}$			$\lambda = (Kl/\pi r\ )(F_{yc}/E)^{.5}$	
		$Cc = (2\pi^2E/F_y)^{.5}$						
	F_y in above eqn is lesser of F_{xe}, F_{xc}, or F_y:			Fy in above eqn is lesser of Fxe, Fxc, or Fy:			F_{yc} in above eqn is given by lesser of expressions below:	
	Local Buckling			Local Buckling			Local Buckling	
F_{xe} =	$2CEt/D$, $C = 0.3$		F_{xe} =	$2C_xEt/D$ $C_x = 0.3$		F_{yc} =	F_y	$F_y/F_{xe}<0.17$
F_{xc} =	$F_y(1.64-0.23(D/t)^{.25})$	D/t>60	F_{xc} =	$Fy(1.64-0.23(D/t)^{.25})$	D/t>60	F_{yc} =	$(1.047-0.274F_y/F_{xe})F_y$	$0.17<F_y/F_{xe}<1.911$
F_{xc} =	F_y	D/t<60	F_{xc} =	F_y	D/t<60	F_{yc} =	F_{xe}	$F_y/F_{xe}>1.911$
						F_{xe} =	$2C_xEt/D$ $C_x = 0.3$	
	BENDING			BENDING			BENDING	
				$f_b <= \phi_b F_{bn}$ (ϕ_b = 0.95)			$f_b <= F_b/\gamma_{Rb}$ (γ_{Rb} =1.05)	
F_b =	$0.75F_y$	D/t<10340/F_y	F_{bn} =	(Z/S)Fy (Z,S Plastic and Elastic Moduli)	D/t<10340/F_y	F_b =	$(Z/S)F_y$	$F_yD/E/t<.0517$
F_b =	$(0.84-1.74F_yD/Et)F_y$	10340/F_y<D/t <20680/F_y	F_{bn} =	$(1.13-2.58F_yD/Et)(Z/S)F_y$	10340/F_y<D/t <20680/F_y	F_b =	$(1.13 - 2.58F_yD/Et)(Z/S)F_y$	$.0517<F_yD/E/t<0.1034$
F_b =	$(0.72-0.58F_yD/Et)F_y$	20680/F_y<D/t <300	F_{bn} =	$(0.94-0.76F_yD/Et)(Z/S)F_y$	20680/F_y<D/t <300	F_b =	$(0.94-0.76F_yD/Et)(Z/S)F_y$	$0.1034<F_yD/E/t<120F_y/E$

* In API RP2A (WSD) the allowable stresses can be increased by 1/3

Table 2.1(b)
Tubular Members Code Provisions

API WSD*			API LRFD			ISO		
Stress/ Parameter	Formulation	Limits	Stress/ Parameter	Formulation	Limits	Stress/ Parameter	Formulation	Limits
	HYDROSTATIC PRESSURE			HYDROSTATIC PRESSURE			HYDROSTATIC PRESSURE	
	$f_h <= F_{hc}/SF_{hc}$			$f_h <= \phi_h F_{hc}$ (ϕ_h = 0.80)			$f_h <= F_h/\gamma_{Rh}$ (γ_{Rh} =1.25)	
F_{hc} =	F_{he}	$F_{he} < 0.55F_y$				F_h =	F_y	$2.44F_y<F_{he}$
F_{hc} =	$.45F_y + .18F_{he}$	$.55F_y<F_{he}<1.6F_y$	F_{hc} =	$0.7F_y(F_{he}/F_y)^{.4}$	$F_{he}>.55F_y$	F_h =	$0.7F_y(F_{he}/F_y)^{.4}$	$.55F_y<F_{he}<2.44F_y$
F_{hc} =	$1.31F_y/(1.15+(F_y/F_{he}))$	$1.6F_y<F_{he}<6.2F_y$	F_h =	F_{he}	$F_{he}<.55F_y$	F_h =	F_{he}	$F_{he}<.55F_y$
F_{hc} =	F_y	$6.2F_y<F_{he}$		$F_{he} = 2C_hEt/d$		F_{he} =	$2C_hEt/D$	
	$F_{he} = 2C_hEt/d$		C_h =	$.44t/D$	1.6D/t<m	C_h =	$.44t/D$	1.6D/t<m
C_h =	$.44t/D$	1.6D/t<M	C_h =	$.44t/D+.21(D/t)^3/m^4$	.825D/t<m<1.6D/t	C_h =	$.44t/D+.21(D/t)^3/m^4$	.825D/t<m<1.6D/t
C_h =	$.44t/D+.21(D/t)^3/m^4$	.825D/t<M<1.6D/t	C_h =	$.737/(m-.579)$	1.5<m<.825D/t	C_h =	$.737/(m - .579)$	1.5<m<.825D/t
C_h =	$.736/(m-.579)$	3.5<M<.825D/t	C_h =	0.8	m<1.5	C_h =	0.8	m<1.5
C_h =	$.755/(m-.559)$	1.5<M<3.5D/t						
C_h =	0.8	M<1.5						
	$M= L/D(2D/t)^{.5}$			$m=L/D(2D/t)^{.5}$			$m=L/D(2D/t)^{.5}$	
	TENSION AND BENDING			TENSION AND BENDING			TENSION AND BENDING	
	$f_a/.6F_y+(f_{bz}^2+f_{by}^2)^{.5}/F_b <1.0$			$1-Cos[(\pi/2)f_t/(\phi_t F_{xc})] + [f_{by}^2 + f_{bz}^2]^{.5}/(\phi_b F_{bn}) <1.0$			$\gamma_{Rt}f_t/F_y+\gamma_{Rb}(f_{by}^2+ f_{bz}^2)^{.5}/F_b <1.0$	
	COMPRESSION AND BENDING			COMPRESSION AND BENDING			COMPRESSION AND BENDING	
	$f_a/F_a+ Cm(f_{bx}^2+fby^2)^{.5}/ [(1-f_a/F'_e)F_b] <1.0$ or			$f_c/(\phi_c F_{cn}) + \{[C_{my}f_{by}/(1-f_c/(\phi_c F_{ey})]^{\epsilon} + [C_{mz}f_{bz}/(1-f_c/(\phi_c F_{ez})]^2\}^{.5}/(\phi_b F_{bn}) <1.0$			$\gamma_{rc}f_c/F_c+\gamma_{rb}[(C_{my}f_{by}/(1-f_c/F_{ey}))^{\epsilon}+(C_{mz}f_{bz}/(1-f_c/F_{ez}))^2)^{.5}/F_b <1.0$	
	$f_a/F_a+ \{(C_{mx}f_{bx}/(1-fa/F'_{ex}))^2+(C_{my}f_{by}/(1-fa/F'ey)^2)\}^{.5}/ F_b<1.0$ and			$1-Cos[(\pi/2)f_c/(\phi_c F_y]+(f_{by}^2+ f_{bz}^2)^{.5}/F_{bn}/\phi_b <1.0$			$\gamma_{Rc}f_c/F_{yc}+\gamma_{Rb}(f_{by}^2+ f_{bz}^2)^{.5}/F_b <1.0$	
	$f_a/.6F_y + (f_{bx}^2 + f_{by}^2)^{.5}/F_b <=1$			$f_c < \phi_c F_{xc}$			$F_{ey} = \pi^2E/(KL/r_y)^2$, $F_{ez} = \pi^2E/(KL/r_z)^2$	

* In API RP2A (WSD) the allowable stresses can be increased by 1/3

Table 2.1(c)
Tubular Members Code Provisions

API WSD			API LRFD			ISO		
Stress/ Parameter	Formulation	Limits	Stress/ Parameter	Formulation	Limits	Stress/ Parameter	Formulation	Limits
	TENSION , BENDING AND HYDROSTATIC PRESSURE			TENSION , BENDING AND HYDROSTATIC PRESSURE			TENSION , BENDING AND HYDROSTATIC PRESSURE (Method A)	
	$A^2 + B^2 + 2\nu\ IAIB <= 1.0$ $A = [(f_t + f_b - (.5f_h))/F_y]SF_x$ $B = [f_h/F_{hc}]SF_h$ $\nu = 0.3$ SF_x = Axial Tension Safety Factor SF_h = Hoop Compression Safety Factor			$A^2 + B^{2\eta} + 2\nu\ IAIB <= 1.0$ $A = [f_t + f_b - (.5f_h)] / (\phi_t F_y)$ $B = f_h/(\phi_h F_{hc})$ $\nu = 0.3$ $\eta = 5\text{-}4F_{hc}/F_y$		If fa >= fq Fth = Fbh = OR, if fa < fq If $f_x > 0.5F_{he}/\gamma_{Rh}$ and $F_{xe}/\gamma_{Rh} > .5F_{he}/\gamma_{Rh}$ Then also : $(\gamma_{Rh}f_h/F_{he})^2 <= 1.0$	$(f_a - f_q)/F_{th} + (f_{by}^2 + f_{bz}^2)^{.5}/F_{bh} <= 1.0$ $F_y((1+0.09B^2-B^{2\eta})^{.5}-0.3B)/\gamma_{Rt}$ $F_b((1+0.09B^2-B^{2\eta})^{.5}-0.3B)/\gamma_{Rb}$ $B = \gamma_{Rh}f_h/F_h$, $\eta = 5 - 4F_h/F_y$ $\gamma_{Rc}\lvert f_a - f_q\rvert/F_{yc} + (f_{by}^2 + f_{bz}^2)^{.5}/F_{bh} <= 1.0$	B<=1.0
	COMPRESSION, BENDING AND HYDROSTATIC PRESSURE $[(f_a + .5f_h)/F_{xc}]SF_x + f_b/F_y\ (SF_b) <= 1.0$ $[f_h/F_{hc}]\ SF_h <= 1.0$ If $f_x > 0.5F_{he}$, then $(f_x - .5F_{ha})/(F_{aa} - .5F_{ha}) + (f_h/F_{ha})^2 <= 1.0$ $F_{ha} = F_{he}/SF_h$ $F_{aa} = F_{xe}/SF_x$			COMPRESSION, BENDING AND HYDROSTATIC PRESSURE Satisfy D.3.2-1, D.3.2-2 and D.3.2-3 and D.2.5-2 and If $f_x > 0.5\ \phi_h F_{he}$, then $(f_x - .5\phi_h F_{he})/(\phi_c F_{xe} - .5\phi_h F_{he}) + (f_h/\phi_h F_{he})^2 <= 1.0$ where $f_x = f_c + f_b + .5f_h$		COMPRESSION, BENDING AND HYDROSTATIC PRESSURE When f_a is compressive $f_a/F_{ch} + ((C_{my}f_{by}/(1-f_a/F_{ey}))^{\zeta} + (C_{mz}f_{bz}/(1-f_a/F_{ez}))^2)^{.5}/F_{bh} < 1.0$ and $\gamma_{Rc}(f_a + f_q)/F_{yc} + (f_{by}^2 + f_{bz}^2)^{.5}/F_{bh} <= 1.0$ F_{ch} = F_{ch} = When f_{ac} is compressive $(f_{ac} - f_q)/F_{ch} + [(C_{my}f_{by}/(1-(f_{ac}-f_q)/F_{ey}))^{\zeta} + (C_{mz}f_{bz}/(1-(f_{ac}-f_q)/F_{ez}))^2]^{.5}/F_{bh} < 1.0$ and $\gamma_{Rc}(f_{ac})/F_{yc} + (f_{by}^2 + f_{bz}^2)^{.5}/F_{bh} <= 1.0$ $\gamma_{Rc}(f_{ac})/F_{yc} + (f_{bv}^2 + f_{bz}^2)^{.5}/F_{bh} <= 1.0$	$.5F_{yc}/\gamma_{Rc}[\zeta\text{-}2f_q/F_{yc} + (\zeta^2 + 1.12\lambda^2 f_q/F_{yc})^{.5}]$ $\zeta = 1\text{-}0.28\lambda^2$ $.9/\lambda^2(F_{yc}/\gamma_{Rc})$	$\lambda < 1.34(1\text{-}2f_q/F_{yc})^{-.5}$ $\lambda >= 1.34(1\text{-}2f_q/F_{yc})^{-.5}$

* In API RP2A (WSD) the allowable stresses can be increased by 1/3

Table 2.2
Statistics for Tubular Members

Database Description	Number of Specimens	Parameter	ISO $\gamma = 1.0$	API LRFD $\phi = 1.0$	ISO γ as given	API LRFD ϕ as given	API WSD* +1/3 overstress
Axial Compression (Local Buckling)	38	Mean bias	1.068	1.121	1.260	1.319	1.398
		COV	0.068	0.060	0.068	0.060	0.060
Axial Compression (Column Buckling)	84	Mean bias	1.063	1.048	1.255	1.233	1.165
		COV	0.045	0.041	0.045	0.041	0.071
Bending	57	Mean bias	1.109	1.109	1.164	1.167	1.432
		COV	0.085	0.085	0.085	0.085	0.087
Hydrostatic Pressure	44	Mean bias	1.142	1.145	1.428	1.431	1.852
		COV	0.124	0.124	0.124	0.124	0.123
Axial Comp. + Bending (Local Buckling)	19	Mean bias	1.251	1.276	1.407	1.434	1.613
		COV	0.066	0.053	0.042	0.035	0.065
Axial Comp. + Bending (Column Buckling)	49	Mean bias	1.029	1.017	1.138	1.147	1.152
		COV	0.082	0.084	0.085	0.084	0.181
Axial Comp. + Bending + Hydrostatic Pressure (Local Buckling)	69	Mean bias	1.294	1.156	1.349	1.359	1.630
		COV	0.155	0.106	0.142	0.097	0.115
Axial Comp. + Bending + Hydrostatic Pressure (Column Buckling)	26	Mean bias	1.252	1.133	1.332	1.291	1.428
		COV	0.112	0.100	0.117	0.095	0.141
Axial Tension + Hydrostatic Pressure	34	Mean bias	1.103	1.103	1.322	1.322	1.793
		COV	0.112	0.112	0.128	0.128	0.108
All data except for previous database (tension & press.)	386	Mean bias	1.138	1.108	1.276	1.280	1.427
		COV	0.134	0.102	0.123	0.114	0.198

* Note: API WSD Safety Factors taken as SFx = 1.25, SFb = 0.75 Fy/Fb and SFh = 1.5

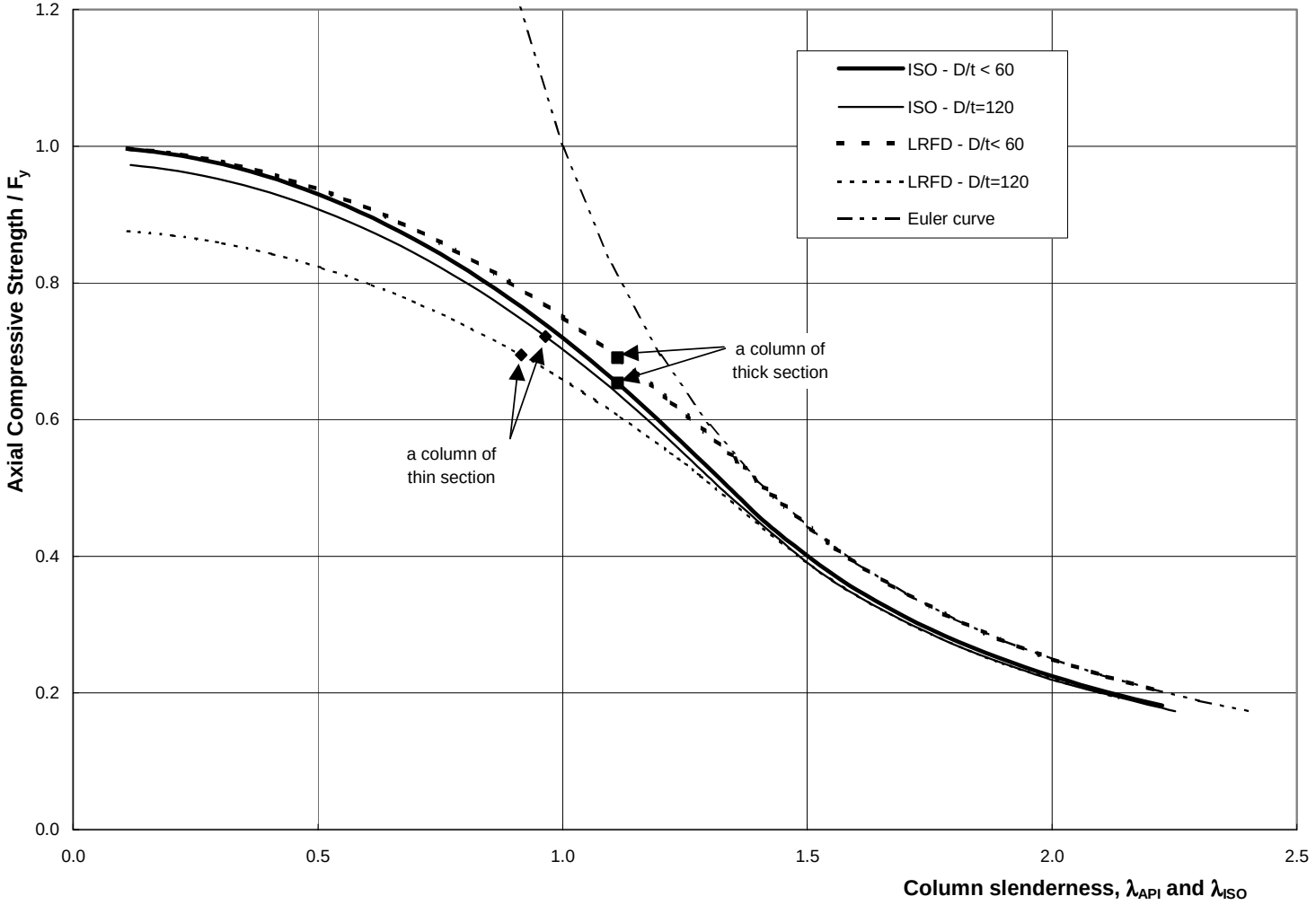

Figure 2.1
ISO and API LRFD Characteristic Column Curves

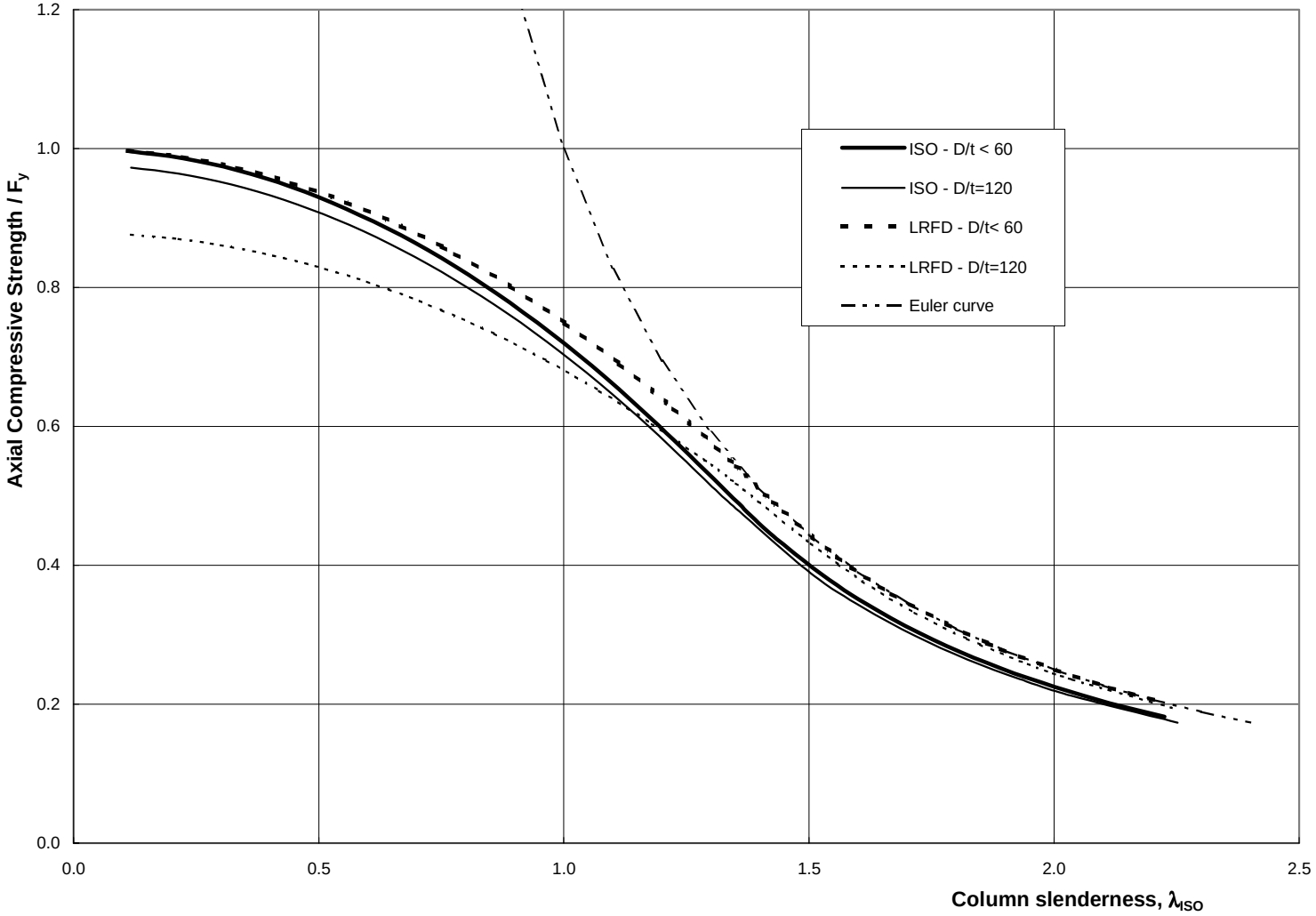

Figure 2.2
Comparison of ISO and API LRFD Characteristic Column Strengths

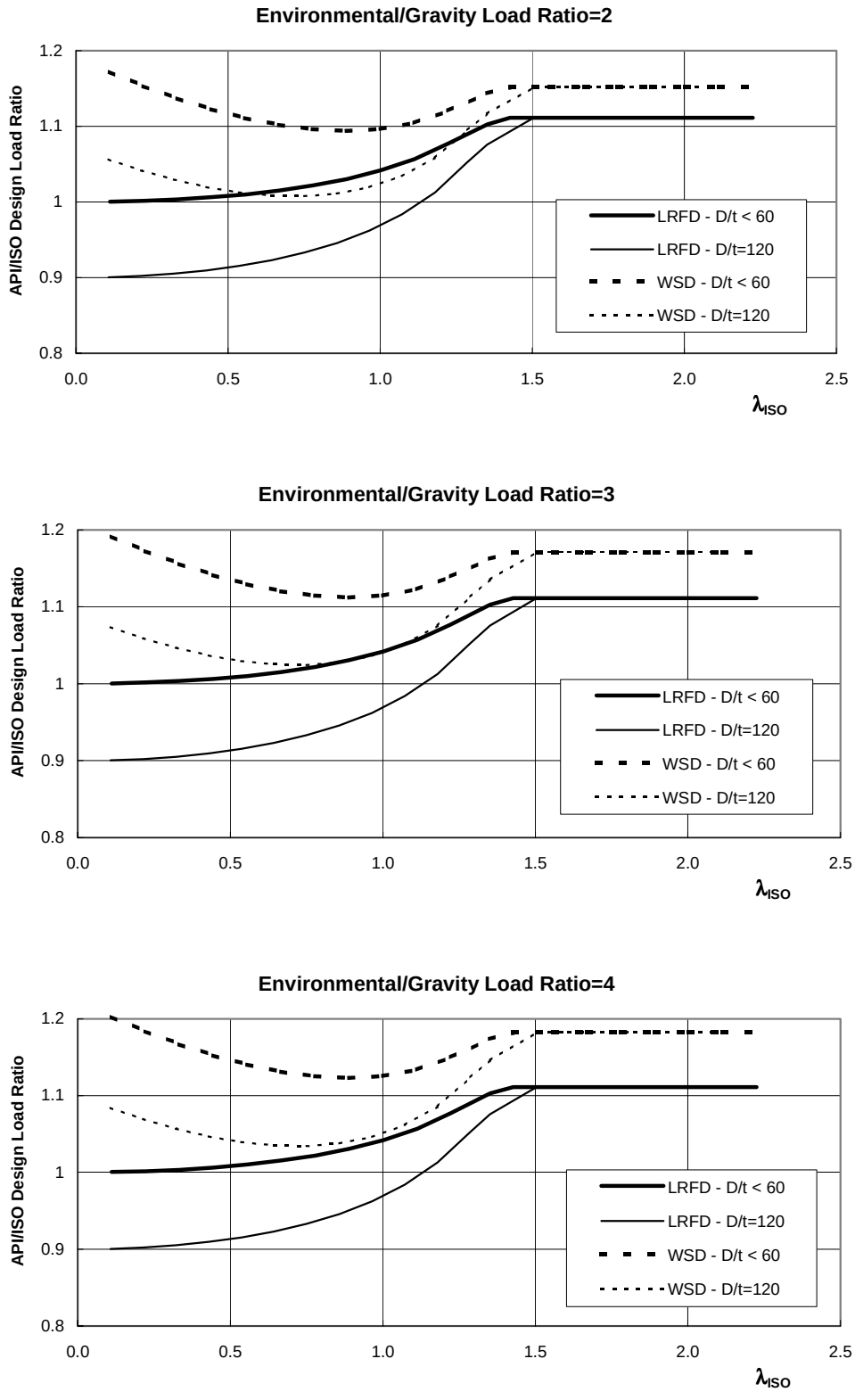

Figure 2.3
Ratio of API (LRFD and WSD) Column Strengths to ISO Column Strength

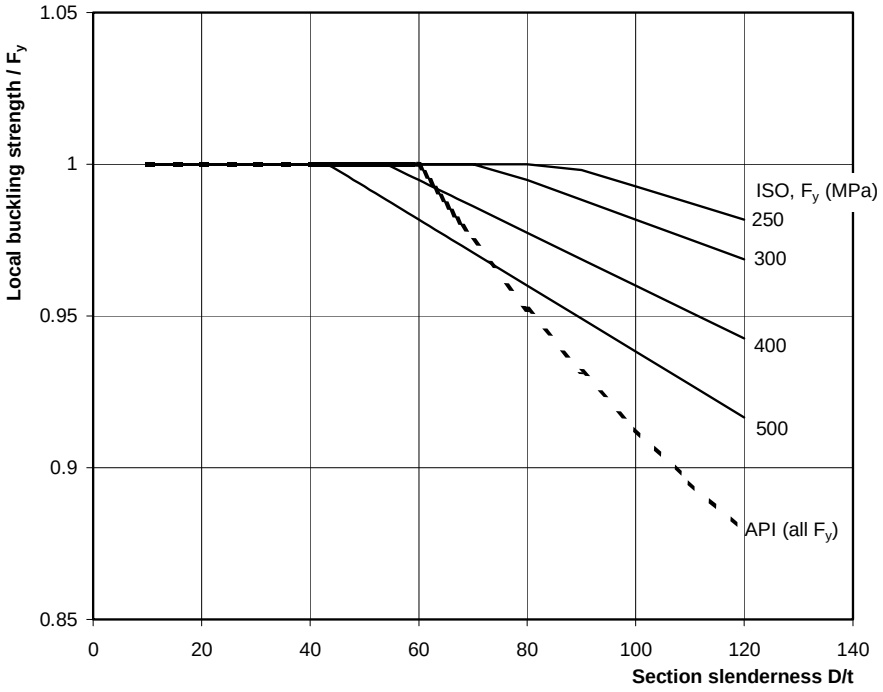

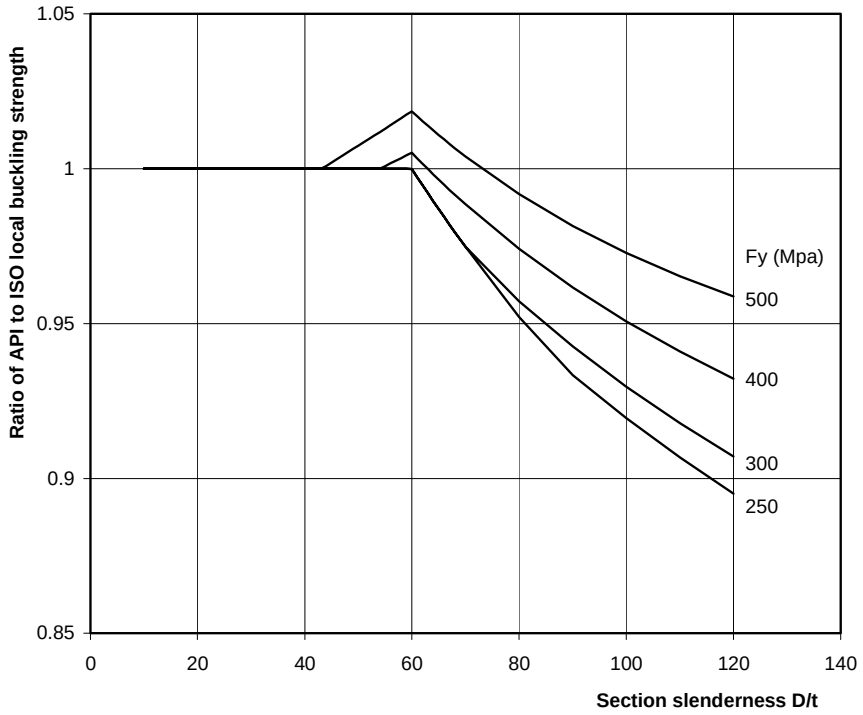

Figure 2.4
Comparison of ISO and API (LRFD or WSD) Local Buckling Strengths

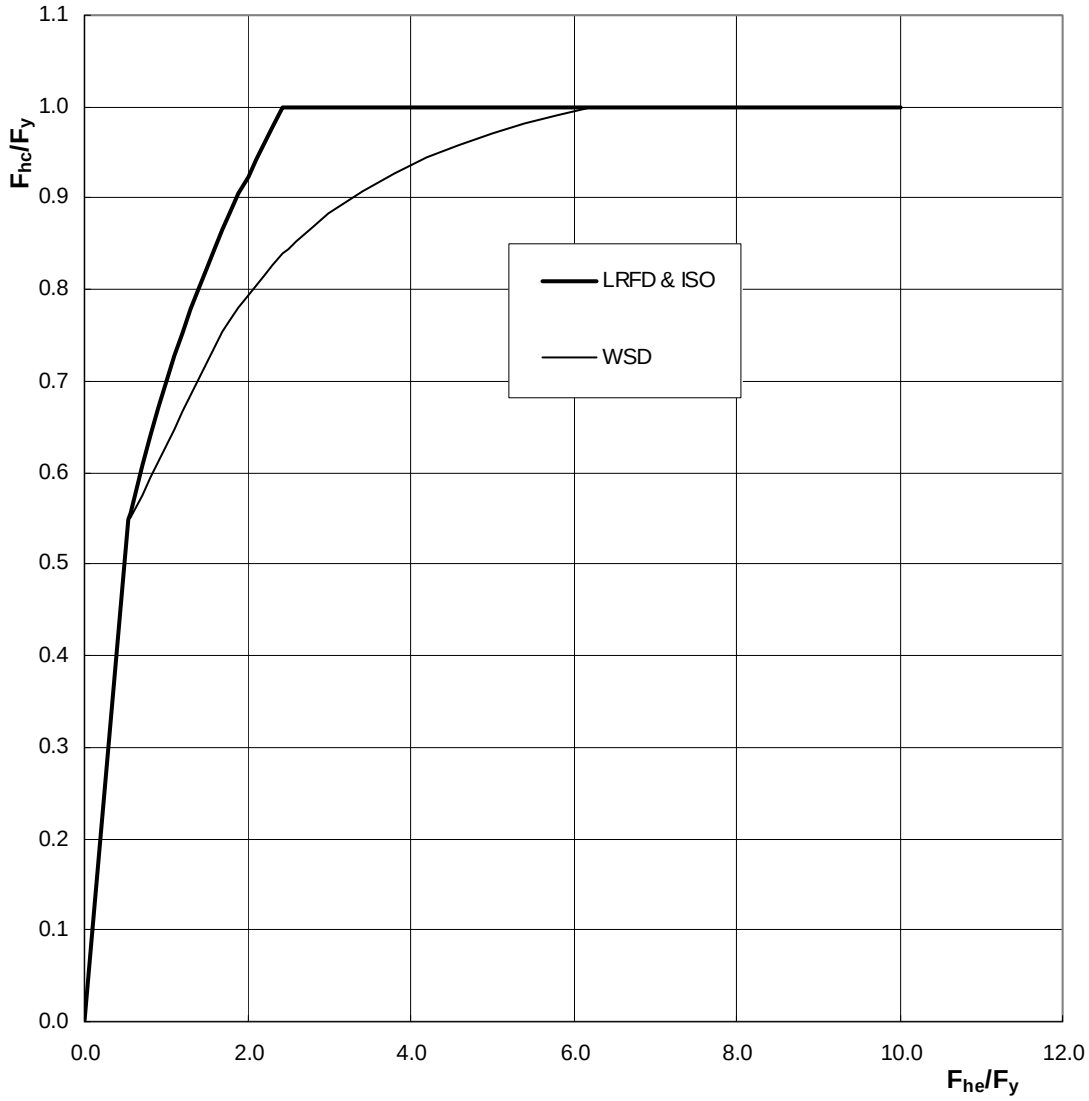

Figure 2.5
Hoop Buckling Strength as a Function of Elastic Buckling Stress

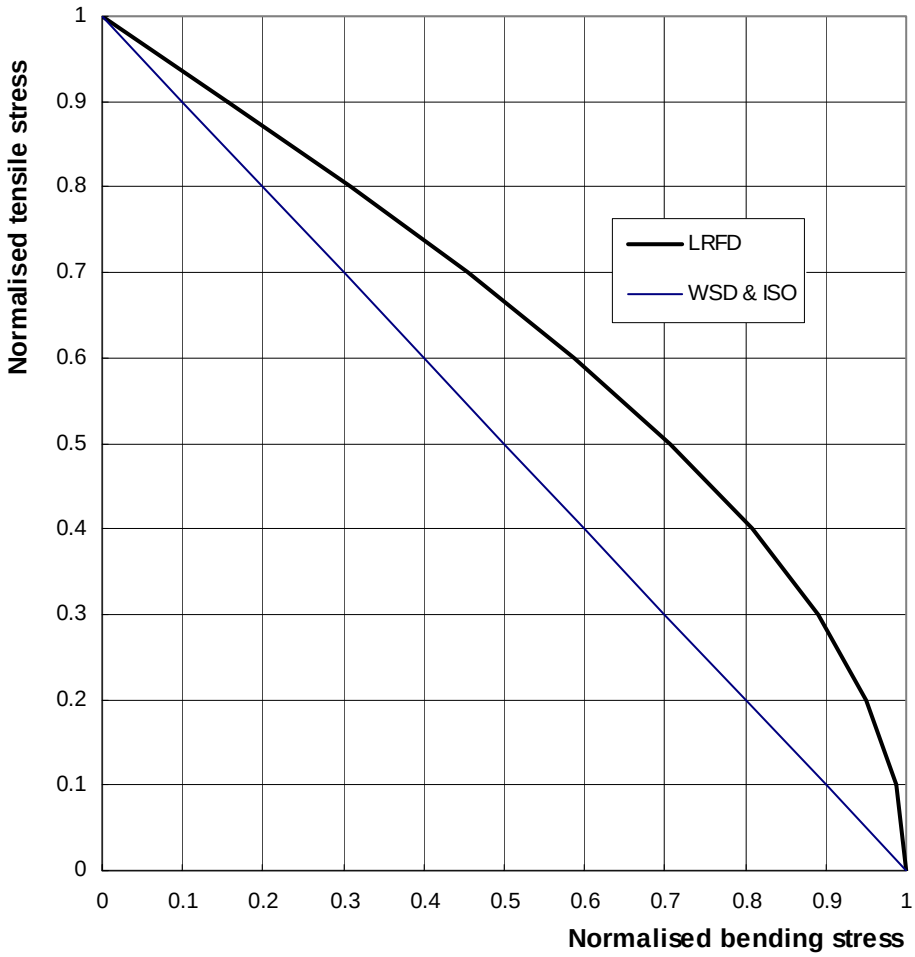

Figure 2.6
Normalised Interaction Curve for Combined Axial Tension and Bending

3. TUBULAR JOINTS

3.1 Code Provisions

The API (WSD and LRFD) and ISO codes follow the same basic procedure for checking the strength of tubular joints. That is the axial capacity and moment capacities are first found from empirical relationships involving non-dimensional factors Q_u and Q_f (the basic strength parameter and a factor accounting for chord loads respectively), and then the joint utilisation is assessed from an interaction equation. The axial capacity is dependent on the weightings of K, Y and X joint actions assigned to the axial load in the brace.

Tables 3.1 and 3.2 summarise and compare the essential provisions of the three codes. The general appearance of these two tables, in that the three columns cover the same ground, emphasises the similarity between the three codes. However, there are differences in detail as noted below.

The API WSD and LRFD practices are almost identical. There is, naturally, a difference in safety factors reflecting the respective working stress and limit state philosophies of the two codes. There is also a difference in the brace interaction equations. The LRFD version does not suffer the same difficulty that the WSD interaction gives when the applied moment is greater than the allowable capacity. However, both versions give the same failure surface (where the joint utilisation is equal to unity).

The ISO brace interaction equation is a simple polynomial expression, rather than the trigonometric formulations in the API codes. It also has a unity exponent on the OPB term in contrast to the squared term in API. This indicates that OPB is considered more damaging in ISO than either of the API practices. These differences are considered further in Section 3.2.

The ISO moment capacity equation does not include the numerical factor of 0.8 that is in the API codes; it has been absorbed into the Q_u factors. The ISO expressions for Q_u are quite different to those in API. These have been mostly derived within the JIP[3.1] executed by MSL and summarised in Reference 3.2. Considerably more data were available to refine the Q_u expressions than when the API expressions were first established. A detailed appraisal of the ISO Q_u values, compared to the API values, is given in Section 3.2. However, it is perhaps noteworthy that overlapped K joints are encompassed within ISO in terms of being assigned a Q_u factor (see Table 3.1).

There are significant differences between the API and ISO Q_f formulations, see Table 3.2. Firstly, there is one of presentation only, in that the 'A' term is expressed as a function of loads in ISO but of stresses in API. Secondly, the dependency of Q_f on γ in API has been removed in the ISO formulation. Thirdly, a variety of 'C' coefficients are included in ISO which adjust the impact of chord loads according to joint type and the nature of the chord load. The consequence of these changes is explored in Section 3.2.

There are three further changes from moving from API to ISO, not addressed in Tables 3.1 and 3.2. These are:

- Short can length

  Both API and ISO cater for the reduced strength if the length of a thickened can is too short (ie. less than 2.5 × chord diameter). In API, the reduction only applies to X joints under axial load whereas in ISO it also applies to Y joints. For the purposes of the present study it can be argued that axially loaded Y joints do not have a significant impact

on overall structural integrity and therefore need not be considered further. As far as X joints are concerned, the presentation of the reduced strength formulation are different in API and ISO but they are in fact equivalent except for joints having $\beta > 0.9$. In this case, ISO recognises that membrane effects come into play such that, at $\beta = 1.0$, the critical can length is reduced to 1.5 times the chord diameter. In other words, ISO gives higher strengths than API for axially loaded, high β, X joints.

- Design Strength (F_y)

  API limits the design strength of the chord material to the yield stress or 2/3 of the ultimate stress if less. In ISO, the 2/3 factor has been relaxed to 0.8. It may be noted that the 2/3 limit begins to govern for 50 ksi (350 MPa) steels. As such, ISO gives marginally higher joint capacities for these and higher strength steels.

- Minimum Capacity

  API requires all joint capacities to be at least 50% of the connected brace strengths (in earthquake regions this rises to 100%). In ISO the minimum capacity requirement is intended to only apply to primary joints that influence the reserve system strength or to secondary joints whose failure has significant safety or environmental consequences. Furthermore, the ISO requirement for such joints is that the calculated interaction ratios of the joints should be at least 15% lower than the subject brace interaction ratios.

3.2 Comparison of Codes

The following compares the provisions of the three codes (API WSD, API LRFD and ISO) and highlights their differences in various figures. It is convenient to examine salient aspects in turn:

- Interaction Curves

  Figure 3.1 illustrates the interaction between in-plane and out-of-plane bending for API (WSD or LRFD) and ISO, in the absence of axial load. For all combinations ISO is more conservative, resulting from the unity exponent (rather than two) on the OPB term.

  For combined axial force and uni-directional moment loading, the interaction curves of ISO straddle that of API, see Figure 3.2. The linear combination in ISO for axial load (P) and OPB gives a curve below that of API, whereas the P + IPB ISO curve is higher than API where the axial load is significant.

  The maximum variation between the ISO and API curves is of the order of 15% but, in practice, will tend to be less than this.

- Basic Strength Factor, Q_u, for Axial Loads

  Figure 3.3 compares the API and ISO Qu factors for joints under axial loading.

  For T/Y joints, no distinction is made in API between compression and tension. In ISO the tension curve is greater than the compression curve. Recognising that gravity loads generally generate compression in members, and that environmental forces generally reverse as a wave passes through a structure, a T/Y joint will usually be governed by its compression capacity. In this instance, the ISO and API compression curves are fairly close although the ISO curve rises above API at $\beta = 1.0$.

Two diagrams are presented for K joints under balanced axial loading, one for $\gamma = 15$ and the other for $\gamma = 30$, these covering the practical range of γ. In each diagram, two values of the gap are considered (g/T = 2 or 5). As can be observed, the greatest differences between ISO and API occur at $\beta = 1.0$.

The differences between ISO and API are most pronounced in the case of X joints having high β values under tension, see lower two diagrams in Figure 3.3. The ISO Qu factor is strongly related to γ at high β (see Table 3.1) and can give double the capacity compared to API.

- Basic Strength Factor, Q_u, for IPB and OPB

  Both ISO and API make no distinction between joint types (K, Y, X) in assigning Qu factors for bending (and therefore there is no need to conduct a moment classification procedure as is required for axial loads).

  Figure 3.4 compares the API and ISO Qu curves for IPB and OPB as given in Table 3.1. The ISO Qu factors are functions of γ. Figure 3.4 would indicate that the API Qu values tend to lie above those of ISO. Whilst this is true, it does not imply higher joint capacities because of the 0.8 factor in the API moment equation (see second line in Table 3.1). A fairer comparison between ISO and API is when the 0.8 factor is included, as shown in Figure 3.5.

- Chord Load Factor, Q_f

  The chord load factor, Q_f, is an important parameter as it directly affects the calculated joint capacity. Despite this observation, it has received relatively little consideration compared to Q_u.

  As noted in Section 3.1, the dependency of Q_f on γ within API has been removed in ISO. Additional changes have been encompassed within ISO for Y/T joints under brace axial loading (leading to chord bending) and K joints under balanced axial loading (resulting in chord axial loading).

  Figures 3.6 to 3.8 compare the API LRFD and ISO Q_f functions for Y, K and X joints respectively. For this purpose the partial safety factor ϕ_q in the 'A' term (see Table 3.2) has been set to unity. In each figure, six diagrams are shown corresponding to the 3×2 matrix : 3 brace load conditions $\times$ 2 chord load conditions (chord IPB and OPB having the same effect in the Q_f formulations). Each diagram plots Q_f against the ratio of chord stress to chord yield stress. Two API curves are shown in each diagram corresponding to $\gamma = 15$ and $\gamma = 30$, a single curve sufficing for ISO as it is independent of γ.

  Most of the diagrams in these three figures are similar with the ISO curve falling in between the API curves for $\gamma = 15$ and 30 (the ISO curve is in fact equivalent to API at $\gamma = 25$). For brace IPB and OPB loading, there is no difference in Q_f, between Y, K or X joints. Apart from the γ-dependency difference noted above, there are really only two changes to the API formulation in ISO. These are the role of chord bending for axially loaded Y joints (see lower left diagram in Figure 3.6) and the role of axial chord loads for K joints under balanced axial loading (see upper left diagram in Figure 3.7). In both cases the influence of chord loads has been reduced in ISO compared to API. These changes have been made following extensive review of available data [Refs. 3.1 and 3.2]. It is shown in the next section how these changes have a significant impact on joint reliability.

3.3 Statistics

In the derivation of design formulations for the static strength of tubular joints, it has been traditional practice to fit Q_u functions to empirical data, without accounting for the effects of chord load (via Q_f) during this stage. Table 3.3 presents the various statistics of test data divided by predicted joint strengths when Q_f is set to unity.

For each of the two limit state codes (ISO and API LRFD), two columns are shown, one relating to setting the partial safety factor to unity and the other to the values cited in the codes. Note that the mean bias is affected by the partial safety factor, whereas the COV is not. Because the WSD and LRFD versions of API are almost identical except for constant factors, then the COVs for given joint and load type are the same for all API columns. (The exception is for overlapped K joints where AISC LRFD and WSD values for shear stress affect the calculated joint capacity differently).

Inspection of Table 3.3 shows that the ISO COV values tend to be lower (ie. better) than those of API, and particularly so for tension loaded Y and X joints.

As mentioned above, joint capacity is dependent on the product of Q_u and Q_f and therefore more pertinent statistics are those derived with the inclusion of chord load effects. Here lies a difficulty in that there are comparatively few data to examine all combinations (3 or 4 brace load types $\times$ 4 chord load types $\times$ 3 joint types gives over 130 combinations). Apart from X joints under brace axial loading, testing arrangements generally lead to some chord load being generated. However, these tend to be small and therefore any chord load effect becomes masked by experimental scatter. Significant chord stresses are induced in axially loaded Y joints (chord bending) and K joints (chord axial load). In these cases it is possible to explore chord load effects. There are also data for DT joints where external chord loads have been applied. These data were used to develop the current API Q_f formulation but are too few in number to establish meaningful statistics.

Table 3.4 considers the effect of chord loads on the statistics for axially loaded Y and K joints. Characteristic biases (defined for 95% survivability at the 50% confidence level) are also provided in the table. The first column under any given code is when Q_f is set to unity and reflects the values given in Table 3.3. The second column, for ISO and API LRFD, incorporates the code Q_f formulation but with all partial factors of safety (including the one in the Q_f term) set to unity. The final column in any given code is with all safety factors included. An inspection of Table 3.4 reveals the following:

- The inclusion of Q_f generally leads to an increase in the mean bias for all codes, but more so in the case of API.

- Whereas the inclusion of Q_f does not significantly affect the ISO COV values (even decreasing it for K joints), the API COVs are substantially increased. (This is due to the manner in which the Q_u and Q_f functions were derived during the development of the two codes.)

- The reliability of the ISO formulations are a great improvement over those of API, as indicated by the characteristic biases being at around unity for the former but sometimes less than unity for the latter.

It may thus be concluded that Q_f may have a significant impact on the statistics. However, the data only permit an investigation of Y and K joints under (brace) axial loading. Actually, the lack of data is not so much of an impediment as it might first appear. This is because system structural integrity, due to design events, is dominated by axial loads in members and

this is where there is greatest confidence in the role of chord load effects. Y and K joints have been examined above, and quantified in Table 3.4. For X joints, there are chord load data and these led to the basic Q_f functions. Furthermore, where no confirmatory data exists, the ISO and API treatment of Q_f is very similar (except for the γ-dependency discussed above). Therefore, on a comparative basis, the uncertainty in Q_f will be more or less equally reflected in ISO and API formulations.

There are three reasons why it is difficult to specify an overall mean bias and a COV for tubular joints.

- No statistics are available for joints subjected to combinations of brace load. As has been seen (Figures 3.1 and 3.2), API and ISO have different formulations for brace load interaction. However, as far as system reliability is concerned, it is expected that brace loads will predominantly be axial, with some in-plane bending.

- Both API and ISO require joints to be 'classified' for the purposes of estimating joint axial capacity. Generally, joints will have various proportions of K, X and Y action, with the capacity assessed according to a weighted averaging procedure. System reliability will be dominated by K or X action in K and X braced frames, and at system ultimate load, the joint classification may approach 100% K and 100% X respectively. In this respect, Y joint statistics become less important.

- The role of chord load effects are relatively poorly researched at present. Yet these can have a significant effect on the statistics, see Table 3.4.

Given the above status, no definitive overall statistics can be given for tubular joints. Nevertheless, the availability of such statistics would be highly desirable for simplifying reliability studies. Therefore tentative values are presented below, based on the above observations and judgements made from Tables 3.3 and 3.4. The values incorporate Q_f and ϕ. It is recognised that alternative statistics may be proposed.

Code	Statistic	X-brace	K-brace
ISO	Mean bias	1.30	1.40
	COV	0.15	0.15
API LRFD	Mean bias	1.35	1.50
	COV	0.20	0.25

Table 3.1
Tubular Joint Code Provisions (General and Qu Factors)

API - WSD	API - LRFD	ISO
$P_a = Q_u Q_f F_y T^2 / (1.7\sin\theta)$ (plus 1/3 increase)	$P_{uj} = Q_u Q_f F_y T^2 / (\sin\theta)$	$P_{uj} = Q_u Q_f F_y T^2 / (\sin\theta)$
$M_a = Q_u Q_f F_y T^2 (0.8\ d) / (1.7\sin\theta)$ (plus 1/3 increase)	$M_{uj} = Q_u Q_f F_y T^2 (0.8\ d) / (\sin\theta)$	$M_{uj} = Q_u Q_f F_y T^2\, d / (\sin\theta)$
	$P_D < \phi_j P_{uj}$ $M_D < \phi_j M_{uj}$	
$(M/M_a)^2_{IPB} + (M/M_a)^2_{OPB} \le 1.0$		
$P/P_a + (2/\pi)\arcsin\{(M/M_a)^2_{IPB} + (M/M_a)^2_{OPB}\}^{0.5} \le 1.0$	$1-\cos\{(\pi/2)P_D/(\phi_j P_{uj})\} + \{(M_D/\phi_j M_{uj})^2_{IPB} + (M_D/\phi_j M_{uj})^2_{OPB}\}^{0.5} \le 1.0$	$P_D/(\phi_j P_{uj}) + \{M_D/(\phi_j M_{uj})\}^2_{IPB} + M_D/(\phi_j M_{uj})_{OPB} \le 1.0$
	ϕ_j = 0.95 except for tension loaded Y and X joints when ϕ_j = 0.90	ϕ_j = 0.95

Joint type	Load type	Q_u
Y	Comp.	$3.4 + 19\beta$
	Tension	$3.4 + 19\beta$
K	Bal. Axial	$(3.4 + 19\beta)Q_g$
X	Comp.	$(3.4 + 13\beta)Q_\beta$
	Tension	$3.4 + 19\beta$
Y,K & X	IPB	$3.4 + 19\beta$
Y,K & X	OPB	$(3.4 + 7\beta)Q_\beta$

$Q_\beta = 0.3/[\beta(1-0.833\beta)]$ for $\beta>0.6$
$= 1.0$ for $\beta\le0.6$

$Q_g = 1.8 - 0.1g/T$ for $\gamma\le20$
$= 1.8 - 4g/D$ for $\gamma>20$
but always $Q_g \ge 1$

Joint type	Load type	Q_u
Y	Comp.	$3.4 + 19\beta$
	Tension	$3.4 + 19\beta$
K	Bal. Axial	$(3.4 + 19\beta)Q_g$
X	Comp.	$(3.4 + 13\beta)Q_\beta$
	Tension	$3.4 + 19\beta$
Y,K & X	IPB	$3.4 + 19\beta$
Y,K & X	OPB	$(3.4 + 7\beta)Q_\beta$

$Q_\beta = 0.3/[\beta(1-0.833\beta)]$ for $\beta>0.6$
$= 1.0$ for $\beta\le0.6$

$Q_g = 1.8 - 0.1g/T$ for $\gamma\le20$
$= 1.8 - 4g/D$ for $\gamma>20$
but always $Q_g \ge 1$

Joint type	Load type	Q_u
Y	Comp.	$(1.9 + 19\beta)Q_\beta^{0.5}$
	Tension	30β
K	Bal. Axial	$(1.9 + 19\beta)Q_\beta^{0.5}Q_g$
X	Comp.	$[2.8 + (12 + 0.1\gamma)\beta]Q_\beta$
	Tension	23β for $\beta\le0.9$ $21 + (\beta-0.9)(17\gamma-220)$ for $\beta>0.9$
Y,K & X	IPB	$4.5\beta\gamma^{0.5}$
Y,K & X	OPB	$3.2\gamma^{(0.5\beta.\beta)}$

$Q_\beta = 0.3/[\beta(1-0.833\beta)]$ for $\beta>0.6$
$= 1.0$ for $\beta\le0.6$

$Q_g = 1.9 - 0.7\gamma^{-0.5}(g/T)^{0.5}$ but≥1, for $g/T\ge2.0$
$= 0.13 + 0.65\psi\gamma^{0.5}$ for $g/T\le-2.0$
= interpolated value for $-2.0< g/T <2.0$

$\psi = t F_{yb}/(T F_y)$

Table 3.2
Tubular Joint Code Provisions (Qf Factors)

API - WSD	API - LRFD	ISO
$Q_f = 1.0 - \lambda \gamma A^2$	$Q_f = 1.0 - \lambda \gamma A^2$	$Q_f = 1.0 - \lambda A^2$
$\lambda = 0.030$ for brace axial load $= 0.045$ for brace in-plane moment $= 0.021$ for brace out-of-plane moment	$\lambda = 0.030$ for brace axial load $= 0.045$ for brace in-plane moment $= 0.021$ for brace out-of-plane moment	$\lambda = 0.030$ for brace axial load $= 0.045$ for brace in-plane moment $= 0.021$ for brace out-of-plane moment
$A = \{f_{AX}^2 + f_{IPB}^2 + f_{OPB}^2\}^{0.5}/(0.6Fy)$ (plus 1/3 increase in denominator)	$A = \{f_{AX}^2 + f_{IPB}^2 + f_{OPB}^2\}^{0.5}/(\phi_q Fy)$ $\phi_q = 0.95$	$A = \{C_1(P_{DC}/P_y)^2 + C_2(M_{DC}/M_p)_{IPB}^2 + C_2(M_{DC}/M_p)_{OPB}^2\}^{0.5}/\phi_q$ $\phi_q = 0.95$ C_1 C_2 Y jts. under brace axial load: 25 11 K jts. under balanced axial load: 14 43 Y & K jts. under brace moment: 25 43 X jts. under any brace loading: 25 43
f_{AX}, f_{IPB} and f_{OPB} are unfactored chord stresses.	f_{AX}, f_{IPB} and f_{OPB} are factored chord stresses.	P_{DC} and M_{DC} (IPB and OPB) are the factored chord axial and moment loads respectively. P_y and M_p are the chord squash load and the chord plastic moment capacity respectively.
Set $Q_f = 1.0$ when all extreme fibre stresses in the chord are tensile.	Set $Q_f = 1.0$ when all extreme fibre stresses in the chord are tensile.	Except for X joints having $\beta > 0.9$, Q_f may be set to unity when all extreme fibre stresses in the chord are tensile.

Table 3.3
Statistics when Qf = 1.0

Joint Type	Brace Loading	Number of Specimens	Parameter	ISO Q_f = 1.0 ϕ_j = 1.0	API LRFD Q_f = 1.0 ϕ_j = 1.0	ISO Q_f = 1.0 ϕ_j = 0.95	API LRFD Q_f = 1.0 ϕ_j = 0.95[1]	API WSD Q_f = 1.0
Y/T	Compression	66	Mean bias	1.265	1.102	1.331	1.160	1.404
			COV	0.131	0.148	0.131	0.148	0.148
	Tension	6	Mean bias	1.708	1.837	1.798	2.042	2.343
			COV	0.239	0.327	0.239	0.327	0.327
	In-plane bending	13	Mean bias	1.213	1.308	1.277	1.377	1.668
			COV	0.106	0.159	0.106	0.159	0.159
	Out-of-plane bending	10	Mean bias	1.268	1.150	1.335	1.210	1.466
			COV	0.118	0.173	0.118	0.173	0.173
X/DT	Compression	72	Mean bias	1.169	1.147	1.230	1.207	1.462
			COV	0.092	0.096	0.092	0.096	0.092
	Tension	11	Mean bias	1.447	1.579	1.523	1.755	2.014
			COV	0.188	0.481	0.188	0.481	0.481
	In-plane bending	5	Mean bias	1.235	1.385	1.300	1.457	1.765
			COV	0.075	0.165	0.075	0.165	0.165
	Out-of-plane bending	4	Mean bias	1.139	1.160	1.199	1.221	1.479
			COV	0.060	0.088	0.060	0.088	0.088
Gapped K joints	Balanced axial	125	Mean bias	1.229	1.333	1.294	1.403	1.700
			COV	0.142	0.150	0.142	0.150	0.150
Overlapped K joints	Balanced axial	55	Mean bias	1.039	1.163	1.093	1.225	1.640
			COV	0.123	0.204	0.123	0.204	0.215
K	In-plane bending	6	Mean bias	1.243	1.287	1.308	1.355	1.641
			COV	0.105	0.095	0.105	0.095	0.095
	Out-of-plane bending	8	Mean bias	1.217	1.164	1.282	1.226	1.485
			COV	0.154	0.142	0.154	0.142	0.142

Note (1): ϕ_j = 0.90 for tension loaded X and Y joints under API LRFD.

Table 3.4
Statistics Including the Effect of Chord Loads

Joint and Load Type	Parameter	ISO			API-LRFD			API-WSD	
		Qf = 1.0 ϕ = 1.0	ISO Qf ϕ = 1.0	ISO Qf ϕ = 0.95	Qf = 1.0 ϕ = 1.0	LRFD Qf ϕ = 1.0	LRFD Qf ϕ = 0.95	Qf = 1.0	WSD Qf
T/Y Compression	Mean	**1.265**	**1.338**	**1.418**	**1.102**	**1.301**	**1.401**	**1.404**	**1.905**
	St. Dev.	0.165	0.202	0.219	0.163	0.347	0.406	0.208	0.843
	COV	**0.131**	**0.151**	**0.154**	**0.148**	**0.267**	**0.290**	**0.148**	**0.443**
	Char.	0.992	1.004	1.056	0.832	0.728	0.730	1.061	0.512
Gapped K Balanced axial	Mean	**1.229**	**1.295**	**1.373**	**1.333**	**1.421**	**1.509**	**1.700**	**1.907**
	St. Dev.	0.174	0.176	0.191	0.200	0.265	0.297	0.255	0.510
	COV	**0.142**	**0.136**	**0.139**	**0.150**	**0.186**	**0.197**	**0.150**	**0.268**
	Char.	0.942	1.005	1.058	1.003	0.984	1.020	1.279	1.066
Overlapped K Balanced axial	Mean	**1.039**	**1.150**	**1.226**	**1.163**	**1.352**	**1.595**	**1.640**	**1.987**
	St. Dev.	0.127	0.100	0.106	0.238	0.332	0.392	0.353	0.609
	COV	**0.123**	**0.087**	**0.086**	**0.204**	**0.246**	**0.246**	**0.215**	**0.307**
	Char.	0.828	0.985	1.051	0.770	0.802	0.946	1.057	0.980

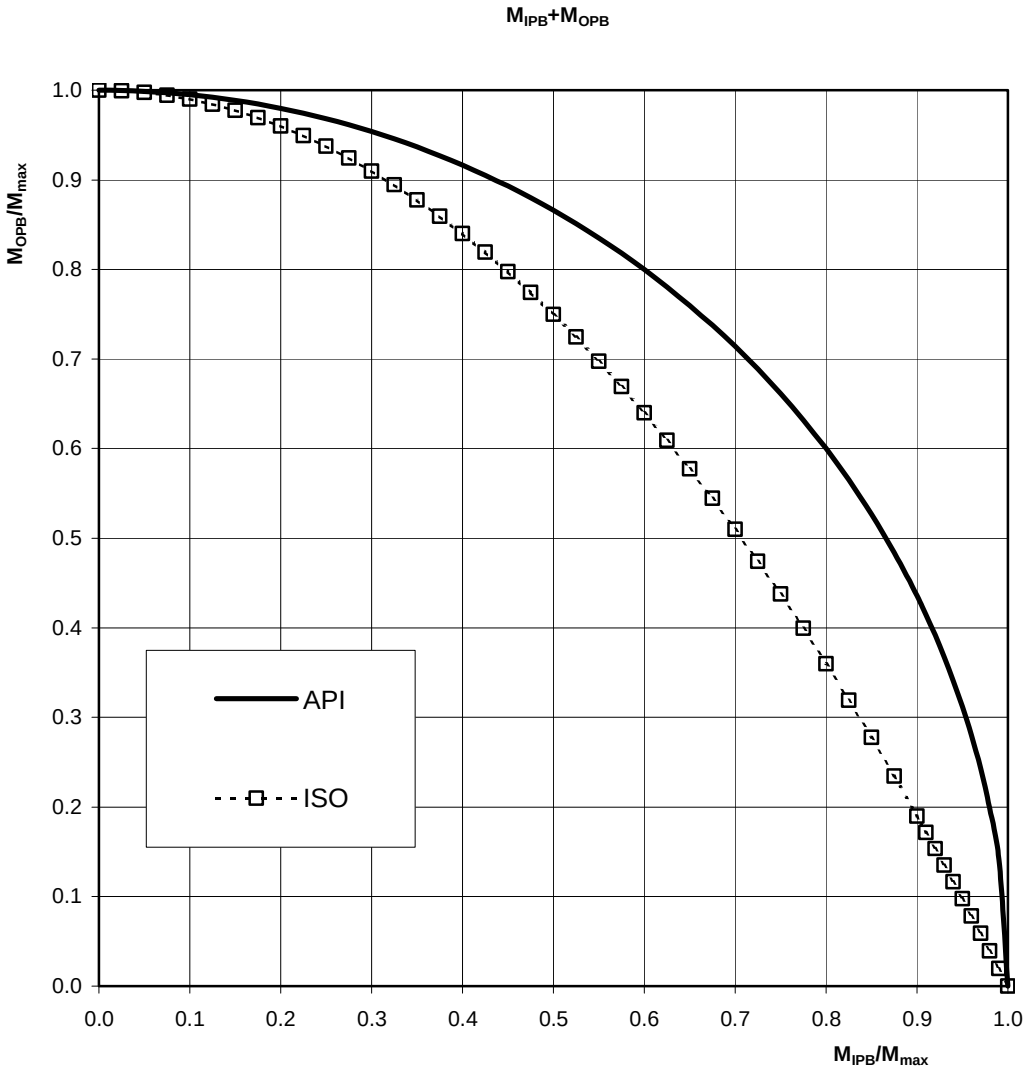

Figure 3.1
Interaction Curves for Tubular Joints under Combined Moment Loading

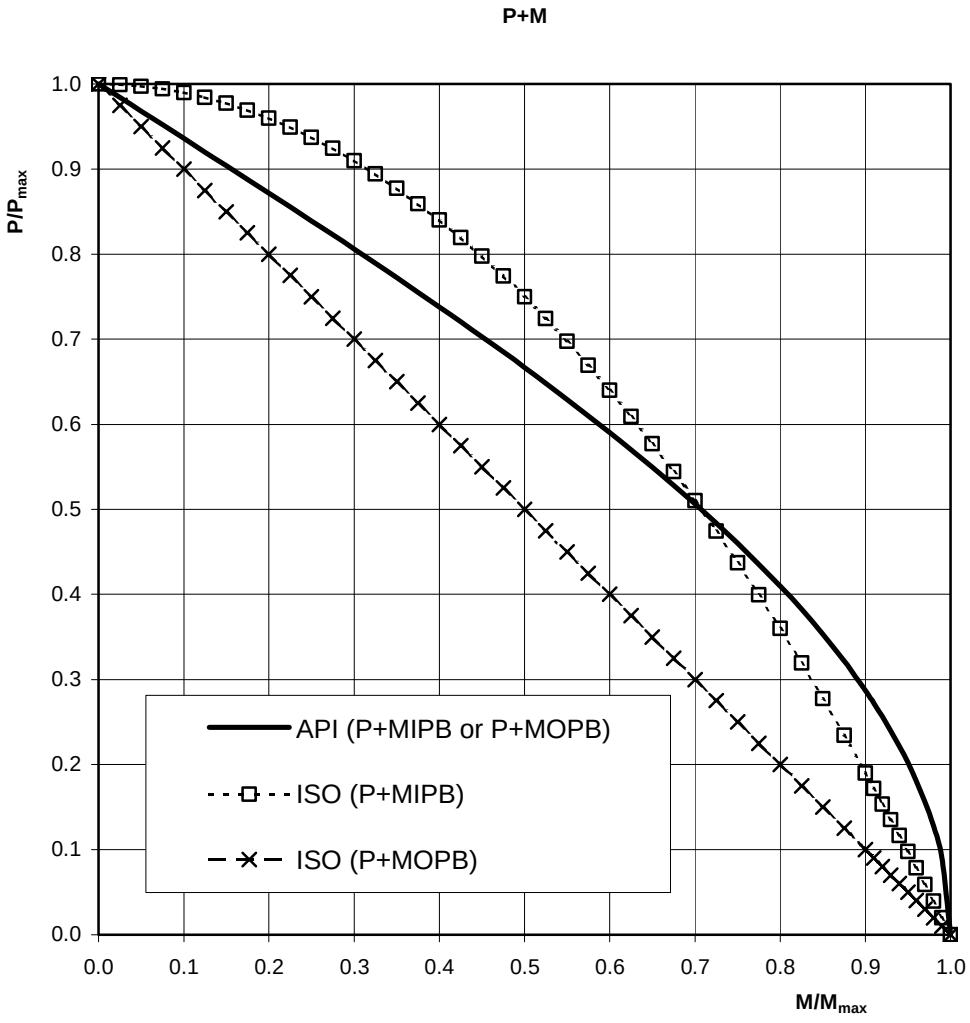

Figure 3.2
Interaction Curves for Tubular Joints under Combined Axial and Uni-Directional Moment Loading

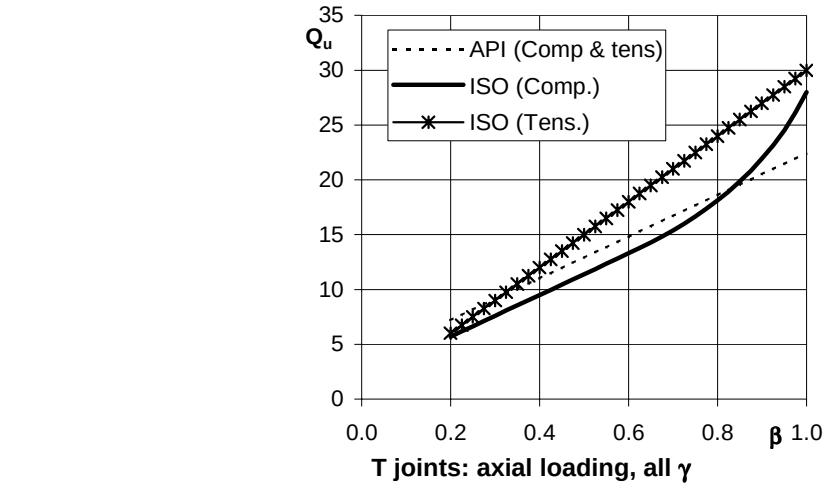

T joints: axial loading, all γ

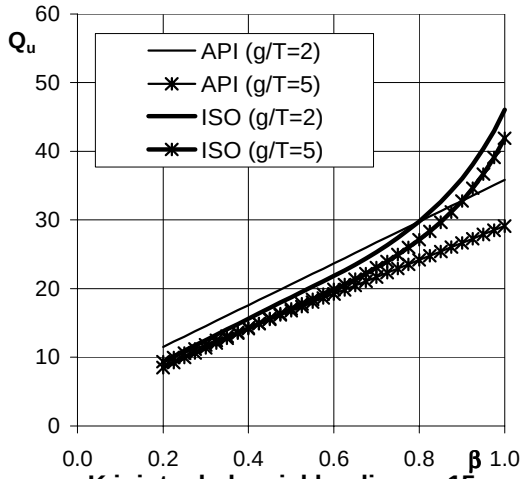

K joints: bal. axial loading, γ=15

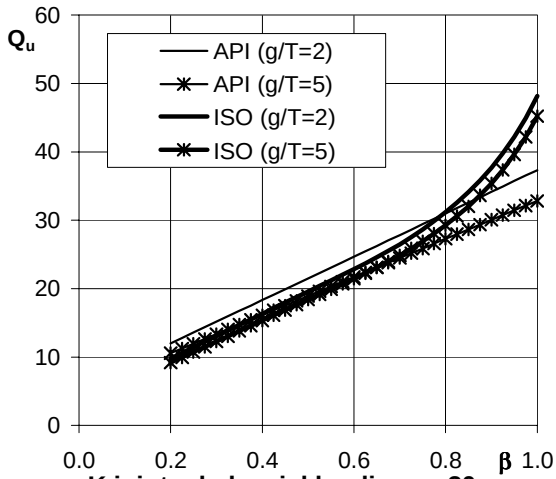

K joints: bal. axial loading, γ=30

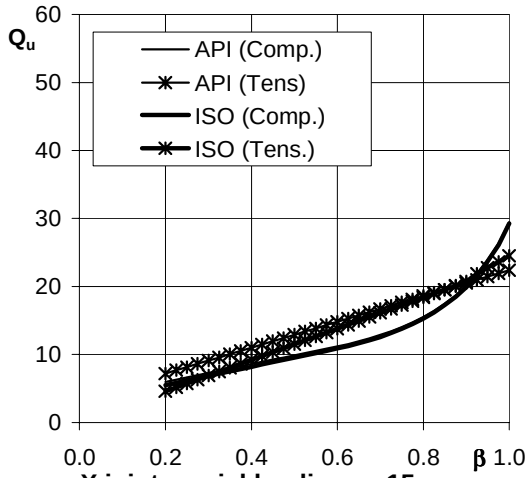

X joints: axial loading, γ=15

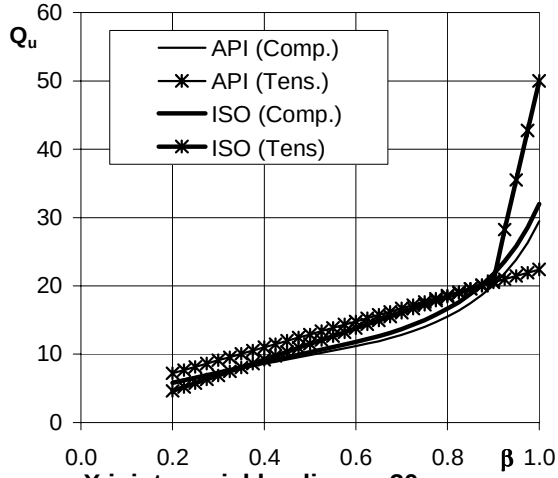

X joints: axial loading, γ=30

Figure 3.3
Comparison of Qu for Axial Loading

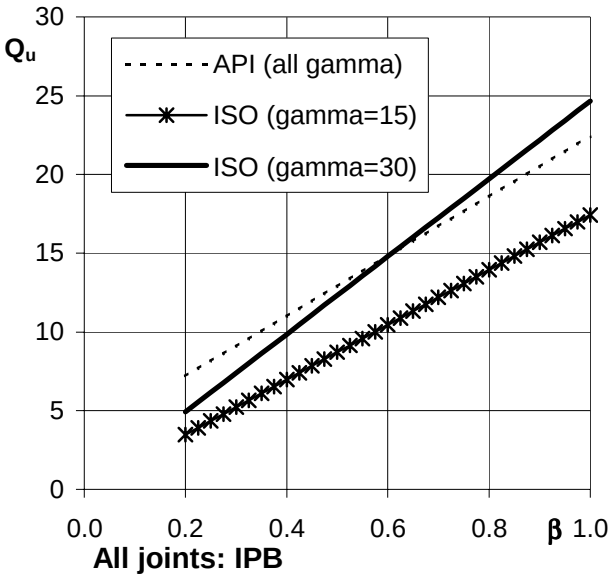

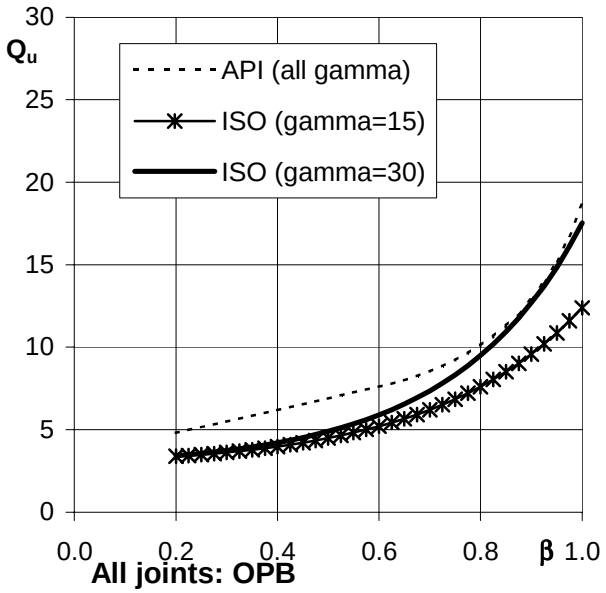

Figure 3.4
Comparison of Q_u for IPB and OPB

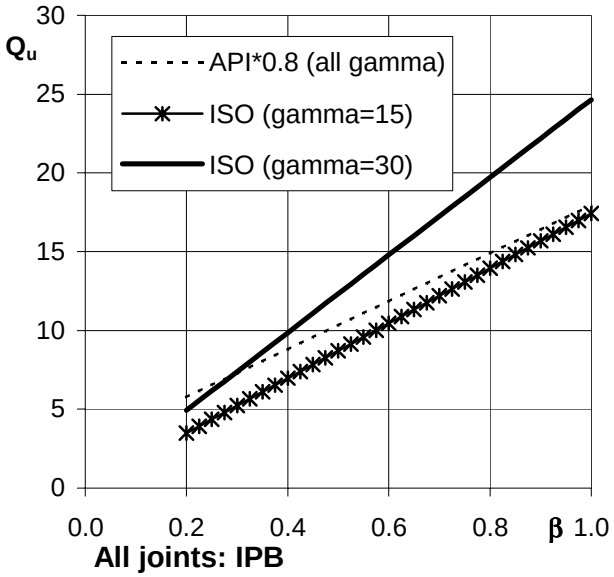

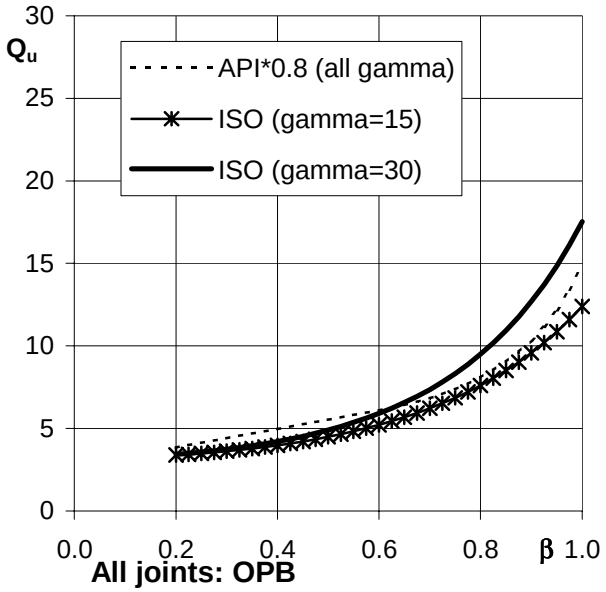

Figure 3.5
Comparison of Qu (ISO) and 0.8 Qu (API) for IPB and OPB

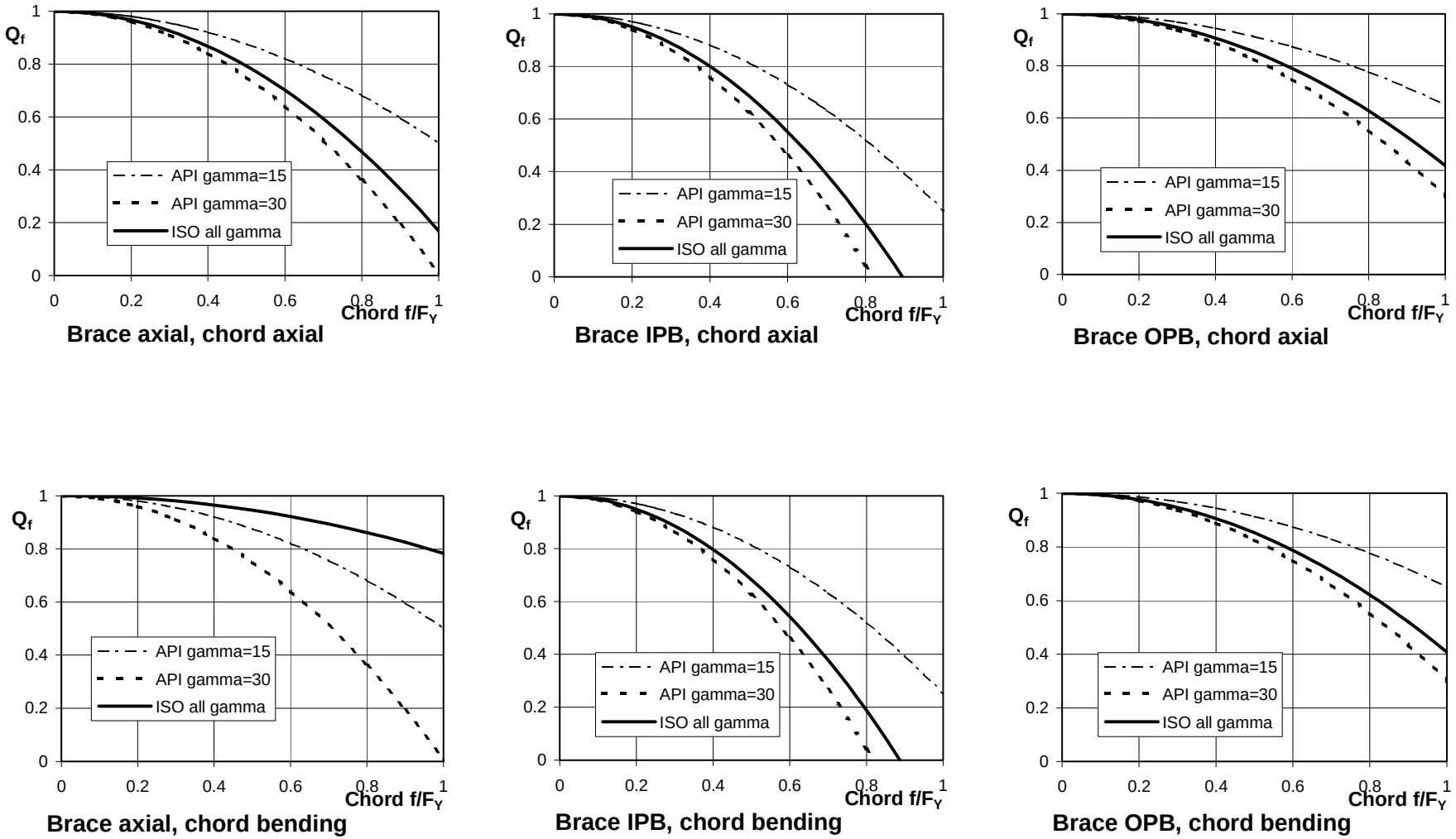

Figure 3.6
Chord Load Factor Qf for Y Joints

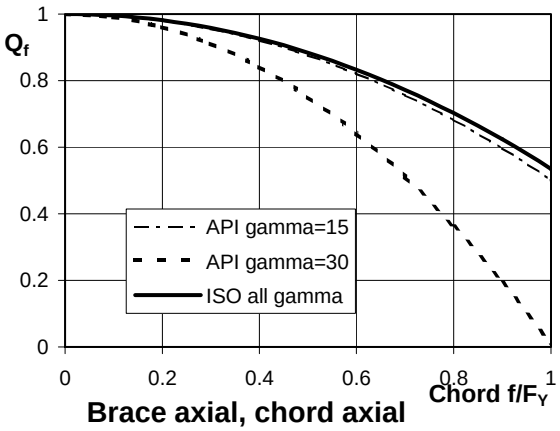

Brace axial, chord axial

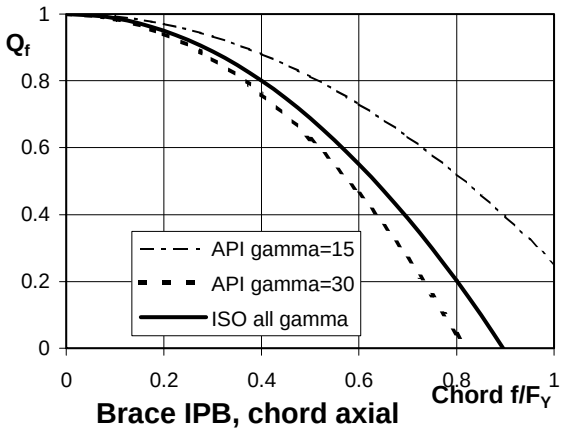

Brace IPB, chord axial

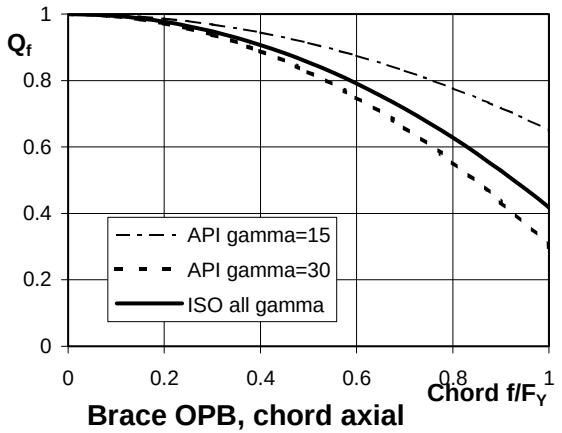

Brace OPB, chord axial

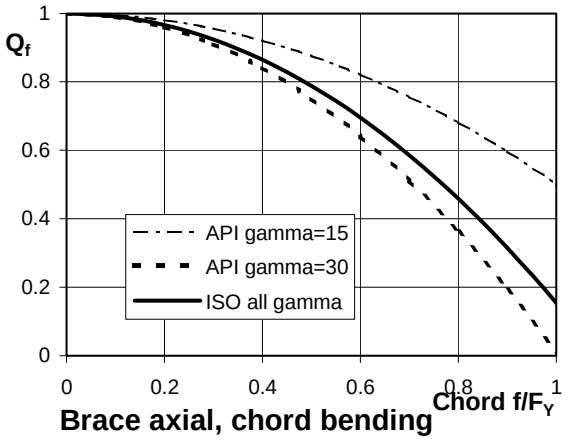

Brace axial, chord bending

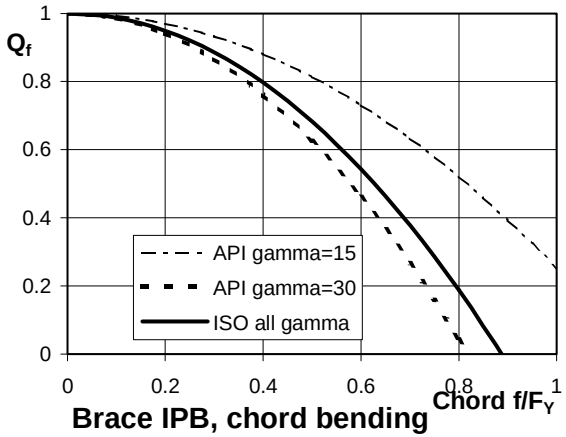

Brace IPB, chord bending

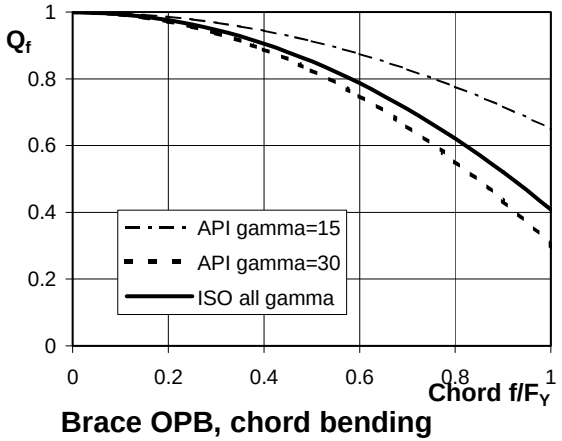

Brace OPB, chord bending

Figure 3.7
Chord Load Factor Qf for K Joints

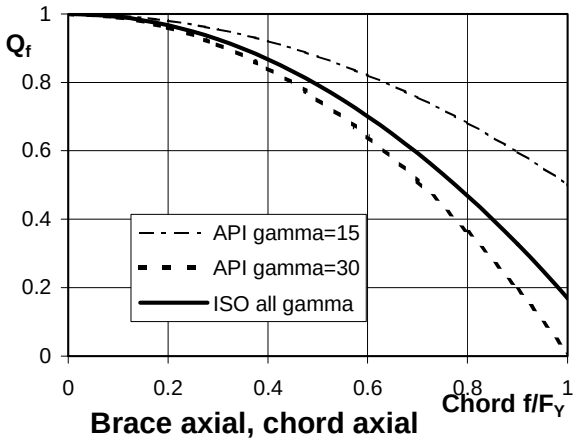

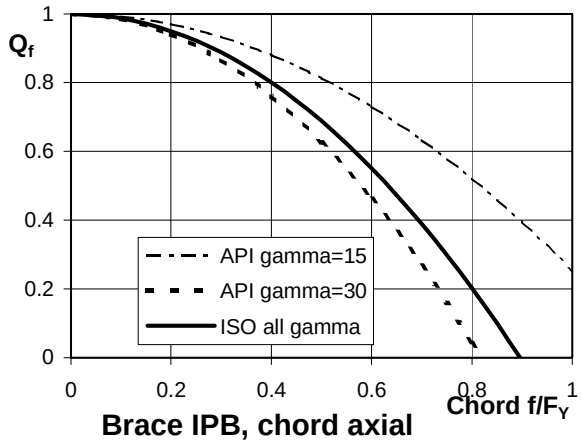

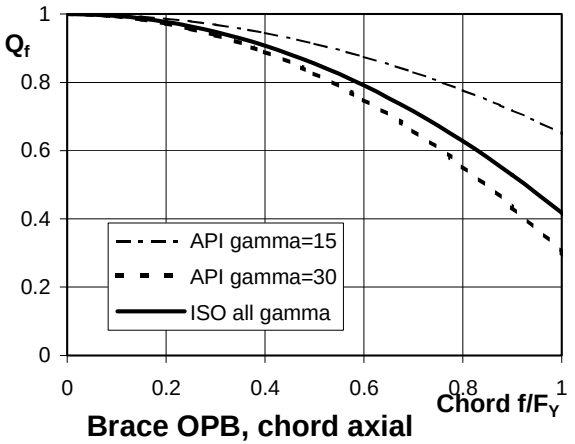

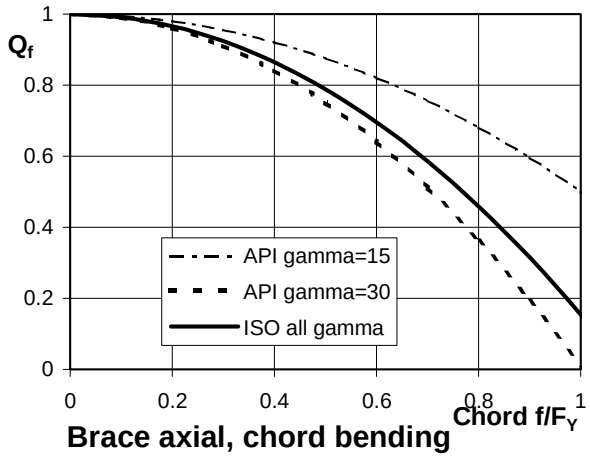

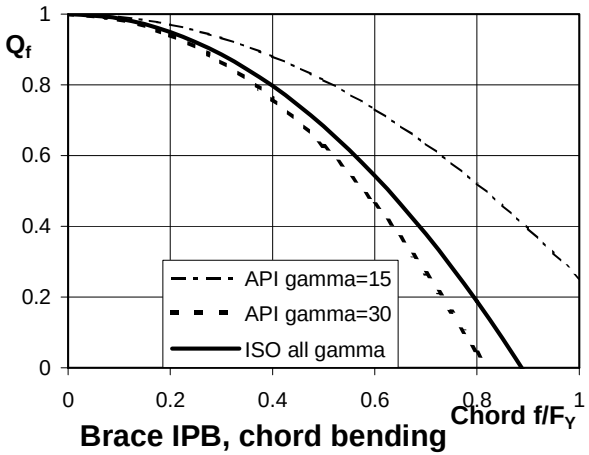

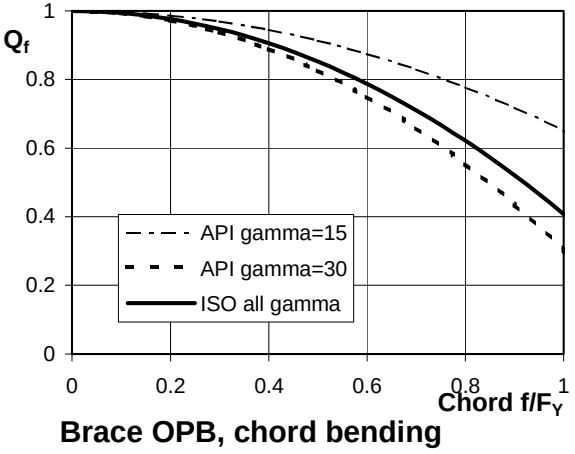

Figure 3.8
Chord Load Factor Qf for X Joints

4. PILE-SLEEVE GROUTED CONNECTIONS

4.1 Code Provisions

Of all the four components which are the subject of this study, it is pile-sleeve connections which have seen the greatest change in code provisions between API and ISO.

The provisions are summarised in Table 4.1. The API WSD and API LRFD provisions are identical except for a constant that reflects the difference between the working stress and the limit state formats. The API equations are fairly simple, the interface transfer strength apparently only being dependent on grout strength and, where weld beads are used, on the bead height to spacing (h/s) ratio. The ISO strength provisions are also functions of a radial stiffness factor (K), and therefore of connection geometry, and a scale correction factor (Cp). Furthermore, there are two criteria to check in ISO, termed grout/steel interface failure and grout matrix failure, whereas API only appears to consider the former.

It may also be observed in Table 4.1 that a much wider range of sleeve geometries is catered for in the ISO provisions. It is also noted that API, though not ISO, has a restriction on the values that f_{cu}.h/s can take. The effect of this restriction is discussed in Section 4.2 below.

The background to the ISO provisions is presented in Reference 4.1.

4.2 Comparison of Codes

The API LRFD and ISO characteristic interface strengths are compared in Figure 4.1. The three diagrams relate to grout cube strengths of 40, 60 and 80N/mm^2. The characteristic strengths have been plotted against the weld bead height to spacing ratio, h/s. Thus, for a plain pipe connection, the strengths are those at h/s = 0.

It can be seen that a family of curves is generated for ISO depending on the radial stiffness parameter K. Only one API curve is required, for a given grout strength, as there is no dependency on K according to the API provisions. The ISO family of curves are limited by the slightly downward sloping line representing grout matrix failure. Although API LRFD does not explicitly cover this failure criterion, it does place a limit on f_{cu}.h/s. This limit is indicated on the lower two diagrams in Figure 4.1. The API curve should therefore properly follow a horizontal line when this limit is reached. In effect this brings about a convergence of the API and ISO strengths.

Figure 4.1 clearly demonstrates that, at the characteristic level, the ISO provisions tend to be more generous than those of API, particularly for lower grout strengths and radially stiffer geometries. However, this is rather negated by a more onerous partial factor of resistance in ISO (0.5 compared with 0.9 in API LRFD).

In order to compare API (LRFD and WSD) with ISO at the design level with both load and resistance factors included, Figure 4.2 was constructed. It shows the ratio of the API design load to that of ISO, where a typical value of environmental/gravity load ratio = 4 is assumed. Again three diagrams are presented to cover a range of grout strengths. As discussed above, the curves are only really valid for h/s ratios less than the indicated API h/s limit.

The API WSD curves follow closely those of API LRFD, typically lying about 10% above. This is not unexpected given that the WSD and LRFD provisions are essentially the same.
In general, there are relatively large discrepancies between ISO and API, by a factor of 2 or more. A factor of 2 implies that a connection designed to the ISO provisions would be twice

as long as one designed to API. However, the ISO Technical Core Group, in setting the partial factor for resistance ($\phi = 0.5$) have taken into account the results of three independent reliability studies (see Reference 4.1) and the relatively poor performance of the API provisions, see Section 4.3.

4.3 Statistics

No information is given in the commentary in ISO on the statistical performance of the provisions. However, the background paper[4.1], supplemented by communications with the ISO Technical Core Group, has provided sufficient details for establishing statistics for ISO and, to a lesser extent, for API.

The screened database used in the development of the ISO provisions contains data on 193 test results. The screened data were used in an assessment of mean strength predictions of various codes, including that of API. The relevant statistics reported in Reference 4.1 are summarised in Table 4.2. It is also reported in the paper that the ISO characteristic to mean ratio was determined as 0.6 for plain pipe connections and between 0.66 and 0.68 for shear key connections, depending on the failure mode. Applying these ratios to the coefficients in the ISO mean strength equations (cited in Table 4.2), one obtains characteristic coefficients 2.1 and 136 for interface failure (rounded to 2 and 140 in Table 4.1), and 0.75 and 1.4 for matrix failure (as given in Table 4.1).

Additional statistics for the API mean strength equation have been provided by C Billington(4.2) with respect to data from an early 1990's UK JIP. The mean bias and COV for the plain pipe data were 0.90 and 0.37 respectively, those for shear key data were 1.27 and 0.35, and those for all data were 1.21 and 0.37. As can be observed, the statistics for the combined data set are very similar to the values reported in Table 4.1, reflecting a similarity in the UK JIP and ISO databases.

The statistics for the ISO factored resistance equation (ie. $\phi.f_{bk}$ as defined in Table 4.1) are summarised in Table 4.3 and were inferred as follows. Taking plain pipe connections first, the mean bias of $\phi.f_{bk}$ is derived as:

$$\text{bias} = \text{mu} \times \frac{m_k}{m_u} \times R / \phi$$

where

m_u	=	mean bias of ISO mean strength equation (= 1.04 from Table 4.1)
m_k/m_u	=	ratio of characteristic/mean biases (= 1/0.60 from Reference 4.1)
R	=	Rounding adjustment (= 2.1/2 as discussed above)
ϕ	=	ISO resistance factor (= 0.5).

Making the substitutions, it is found that the mean bias for plain pipe connections is 3.64. The COV quoted in Table 4.2 for plain pipe connection is still relevant as there is only a numerical factor difference between the mean and characteristic plain pipe equations. Thus, the COV for plain pipe connections remains at 0.29.

For connections with shear keys, a similar procedure was used but without applying the rounding adjustment, R (as the first term in the equation was rounded down but the second term up). The mean bias of $\phi.f_{bk}$ for shear key connections was therefore calculated as $1.00 / (0.68 \times 0.5) = 2.94$. Inspection of Table 4.2 would suggest that the database is dominated by shear key specimens suffering interface failure for which the COV is 0.19.

There is insufficient information in References 4.1 to 4.3 to derive corresponding statistics for API. The fact that the API characteristic strength equation (Table 4.1) is not simply the mean strength equation (Table 4.2) times a numerical factor, limits what can be done.

Table 4.1
Code Provisions for Grouted Pile-Sleeve Connections

API - WSD	API - LRFD	ISO
$f = P/(\pi D_p L) \leq f_{ba}$	$f = P_d/(\pi D_p L) \leq \phi.f_{ba}$	$f = P_d/(\pi D_p L) \leq \phi.f_{bk}$
where:	where:	where:
P = Unfactored Load	P_d = Factored Load	P_d = Factored Load
	ϕ = 0.9	ϕ = 0.5
$f_{ba} = 0.184 + 0.67*f_{cu}*(h/s)$	$f_{ba} = 0.248 + 0.90*f_{cu}*(h/s)$	$f_{bk} = C_p*[2 + 140*(h/s)^{0.8}]*K^{0.6}f_{cu}^{0.3}$ or $[0.75\text{-}1.4*(h/s)]*f_{cu}^{0.5}$ (whichever is the smaller)
		$C_p = (D_p/1000)^2 - D_p/500 + 2$ for $D_p < 1000$mm $= 1.0$ for $D_p > 1000$mm
		$K = [D_p/t_p + D_s/t_s]^{-1} + (1/m)*(D_g/t_g)^{-1}$
<u>API Limits</u>		<u>ISO Limits</u>
17 MPa ≤ f_{cu} ≤ 110 MPa		10 MPa ≤ f_{cu} ≤ 80 MPa
h/s ≤ 0.10		h/s ≤ 0.10
$f_{cu}*h/s$ ≤ 5.5 MPa		
D_s/t_s ≤ 80		30 ≤ D_s/t_s ≤ 140
D_p/t_p ≤ 40		20 ≤ D_p/t_p ≤ 40
7 ≤ D_g/t_g ≤ 45		10 ≤ D_g/t_g ≤ 50
D_p/s ≤ 8		D_p/s ≤ 12
1.5 ≤ w/h ≤ 3		
		h/D_p ≤ 0.012
		K ≤ 0.02
		1 ≤ L_e/D_p ≤ 10

Table 4.2
Statistics for Mean Strength Equations as Reported in Reference 4.1

Database	Equation	Mean Bias	COV
All data	ISO - Mean $f_{bu} = C_p[3.5C_s + 200(h/s)^{0.8}] K^{0.6} f_{cu}^{0.3}$ or $[1.1 - 2*(h/s)] f_{cu}^{0.5}$ if smaller	0.99	0.19
Plain pipe only	ISO - Mean	1.04	0.29
Shear key -interface failure	ISO - Mean	0.98	0.19
Shear key -matrix failure	ISO - Mean	1.02	0.23
All data	API LRFD - Mean (4.3) $f_{bu} = 1.15 + 1.72 f_{cu} (h/s)$	1.21	0.35

Table 4.3
Inferred Statistics for Factored ISO Characteristic Equation

Database	Equation	Mean Bias	COV
Plain pipe only	ISO - Factored Characteristic $\phi.f_{bk} = 0.5C_p[2 + 140(h/s)^{0.8}] K^{0.6} f_{cu}^{0.3}$ or $0.5[0.75 - 1.4*(h/s)] f_{cu}^{0.5}$ if less	3.64	0.29
Shear key		2.94	0.20

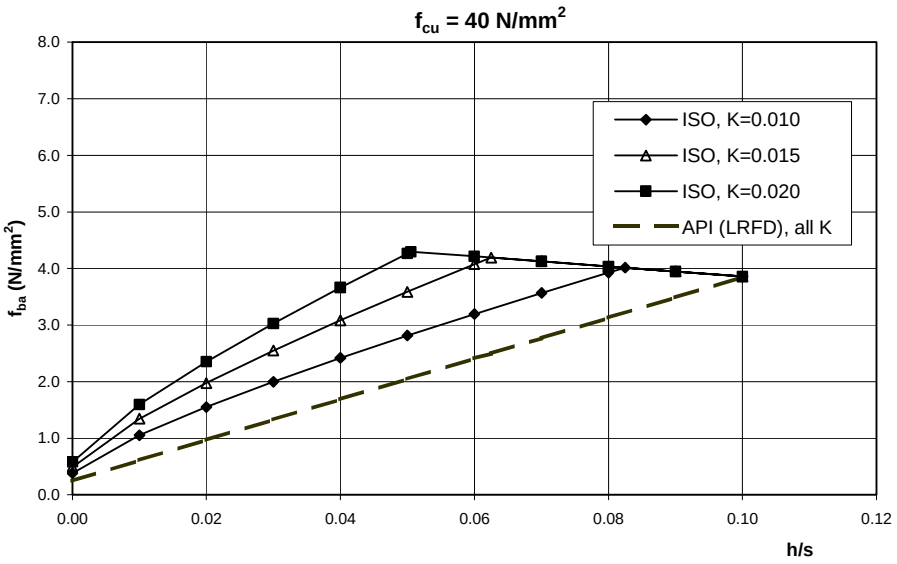

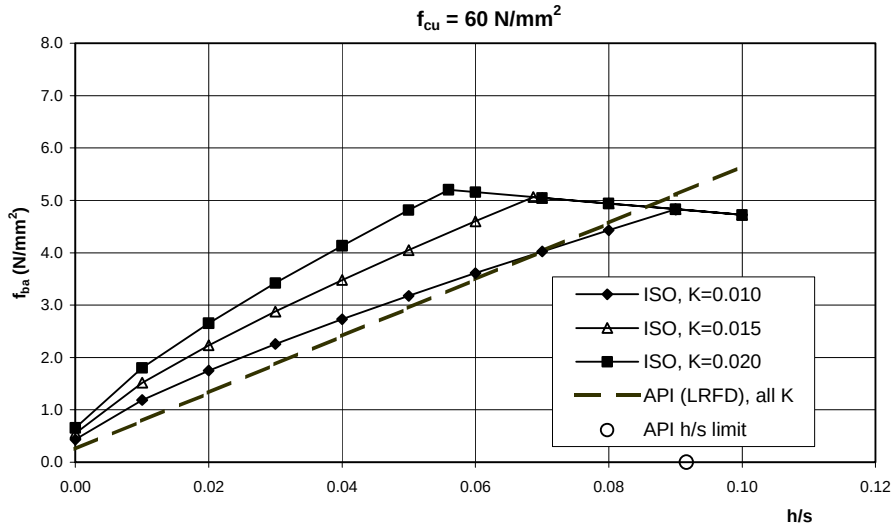

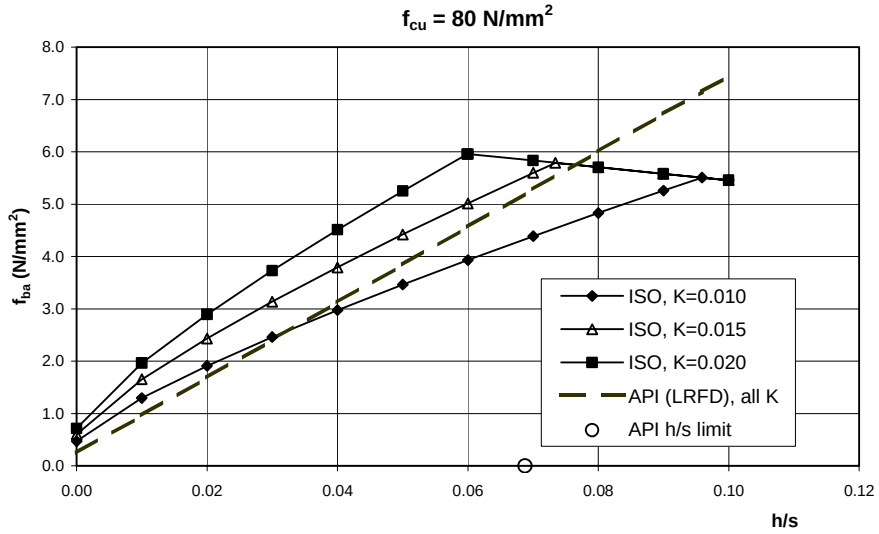

Figure 4.1
Comparison of ISO and API Characteristic Interface Transfer Strengths

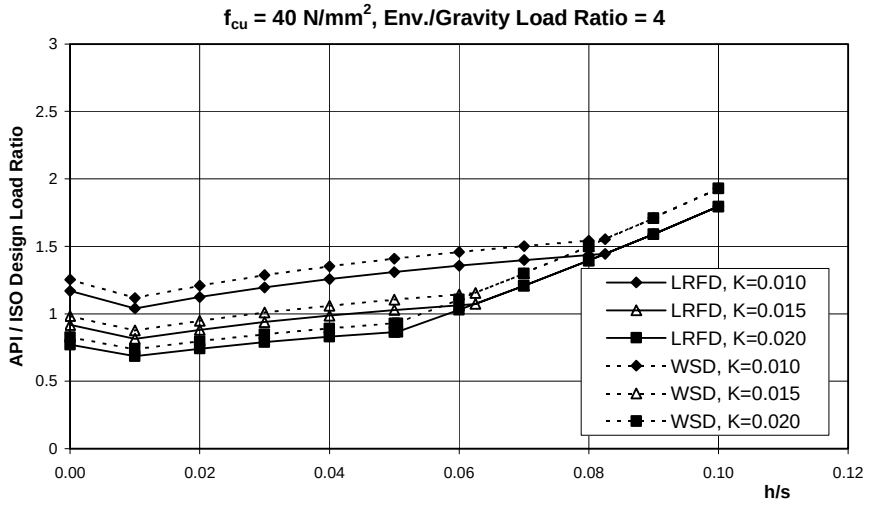

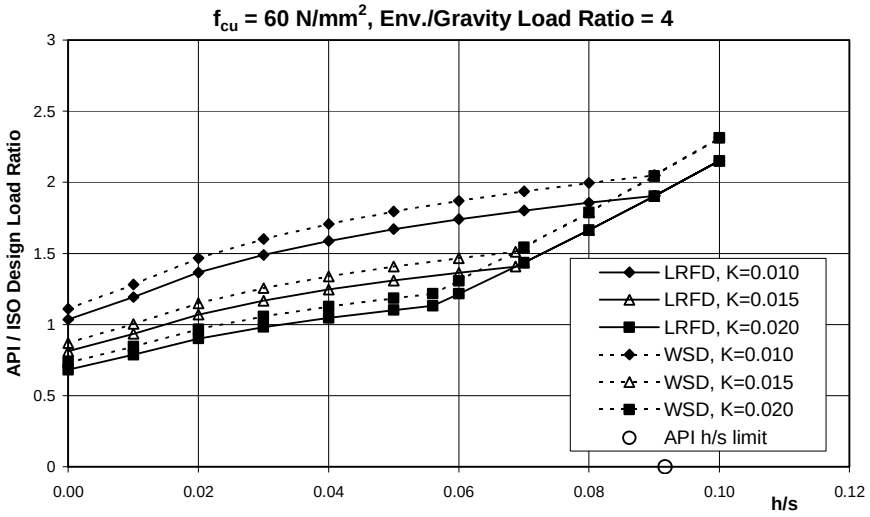

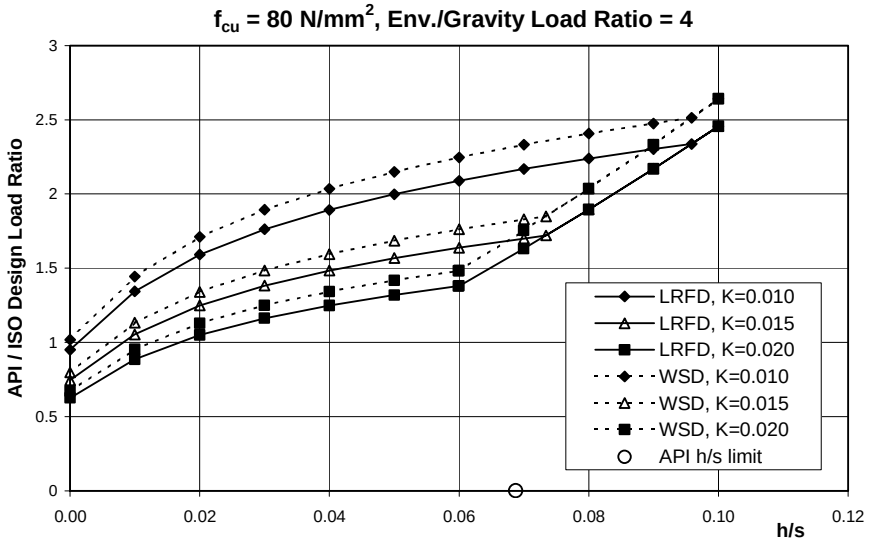

Figure 4.2
Ratio of API to ISO Design Capacities

5. PILE CAPACITY

5.1 Code Provision

The API and ISO code provisions for estimating pile capacity are almost identical, see Table 5.1. There are some differences in factors of safety, though not between API LRFD and ISO for extreme environmental conditions, and in some of the recommended values for the parameters to use in estimating capacities in cohesionless soils.

ISO introduces clayey sand as a soil classification but omits silts and gravels. There are, too, some issues related to classification terminology when comparing API and ISO, ie. "sand-silt" is used in API whereas ISO uses "silty sand" and "sandy silt". However, in general, API and ISO generally agree on the soil classification scheme.

The most significant difference is considered to lie with the recommended values for K, the ratio of horizontal to vertical effective stress, see Table 5.1. The ISO values for piles under tension loading are significantly less (by up to 30% and 37% for closed and open ended piles respectively) than the API values.

5.2 Comparison of Codes

Given the broad similarity of the three codes with respect to pile capacity provisions, there needs little comment here. It was noted above that the most significant difference concerns the K parameter. This parameter directly affects the estimate of pile shaft friction in cohesionless soils. For piles in tension, shaft friction is the only line of resistance and therefore ISO pile capacity estimates would be about 25% lower than API estimates. For piles in compression, K would be reduced by about 10% but in this case end bearing contributes to pile resistance. A fairly typical pile design would have end bearing contributing about 25% to pile resistance. On this basis the ISO compression capacity would be about 7.5% lower than that of API. It may be noted that compression capacity normally governs pile design except where the structure is lightweight (eg. as in minimal structures).

5.3 Statistics

No statistics are quoted in any of the three codes. Although pile load test data exist they do not appear to be collated into a readily available form in the public domain. It is therefore not possible within the context of this study to present statistics.

Nevertheless, it is noted that API and ISO essentially have the same provisions for pile capacity, and therefore will have similar statistics for use in comparative studies. Because of the difference in the K parameter leading to lower ISO pile capacity estimates in cohesionless soils, the mean bias for ISO (measured over predicted strength) will be slightly higher for ISO than API, by a factor of around 1.07.

Table 5.1
Code Provisions for Pile Capacity

API - WSD	API - LRFD	ISO
$P_D \le Q_D / \gamma$	$P_D \le \phi_P Q_D$	$P_D \le Q_D / \gamma_P$
where:	where:	where:
γ = 1.5 for ext. Env. + drilling		
γ = 2.0 for op. Env. + drilling	ϕ_P = 0.8 for extreme Env. (=1/1.25)	γ_P = 1.25 for extreme Env.
γ = 1.5 for ext. Env. + producing	ϕ_P = 0.7 for operating Env. (=1/1.43)	γ_P = 1.50 for static load conditions
γ = 2.0 for op. Env. + producing		
γ = 1.5 for ext. Env. (tension)		

The provisions for evaluating Q_D are the same for all three codes and are:

$Q_D = Q_f + Q_p = f A_s + q A_p$ (for compression)

$Q_D = Q_f = f A_s$ (for tension)

a) Cohesive Soils

$f = \alpha c$

$\alpha = 0.5 \psi^{-0.5}$ but ≤ 1.0, for $\psi \le 1.0$

$= 0.5 \psi^{-0.25}$ for $\psi > 1.0$

$\psi = c/p'_o$

c = Undrained shear strength

p'_o = Eff. overburden pressure

$q = 9 c$

b) Cohesionless Soils

$f = K p'_o \tan \delta$

K = Ratio of horiz./vert. effective stress

p'_o = Eff. overburden pressure

δ = Friction angle between soil & pile wall

$q = p'_o N_q$

N_q = Non-dimensional bearing capacity factor, tabulated in the code

Notes: 1. For both soil types, p'_o should be evaluated at the point in question

2. For open-ended piles under compression, internal skin friction not to exceed plug bearing

3. For pull-out conditions, weight of soil plug can be included where justified.

For cohesionless soils, there are differences between API (WSD or LRFD) and ISO w.r.t. values of K and certain parameters depending on soil classification:

	API	ISO
K values for		
Open ended piles under compression loading:	0.8	0.7 - 0.8
Open ended piles under tension loading:	0.8	0.5 - 0.7
Closed ended piles under compression loading:	1.0	0.8 - 1.0
Closed ended piles under tension loading:	1.0	0.7 - 0.8
		(Higher values relate to denser materials)

Soil classification (type & density):	δ values (deg.)		Limiting f (kPa)		N_q		Limiting q (MPa)	
	API	ISO	API	ISO	API	ISO	API	ISO
Sand - very loose	15	-	47.8	-	8	-	1.9	-
- loose	20	20	67.0	65	12	12	2.9	3
- medium	25	25	81.3	80	20	20	4.8	5
- dense	30	30	95.7	95	40	40	9.6	10
- very dense	35	35	114.8	115	50	50	12.0	12
Silty sand - loose	15	20	47.8	65	8	12	1.9	3
- medium	20	20	67.0	65	12	12	2.9	3
- dense	25	-	81.3	-	20	-	4.8	-
- very dense	30	-	95.7	-	40	-	9.6	-
Clayey sand - dense	-	25	-	80	-	20	-	5
- very dense	-	30	-	95	-	40	-	10
Sandy silt - loose	-	15	-	45	-	8	-	2
- medium	-	20	-	65	-	12	-	3
- dense	25	20	81.3	65	20	12	4.8	3
- very dense	30	25	95.7	80	40	20	9.6	5
Silt - medium	15	-	47.8	-	8	-	1.9	-
Gravel - dense	35	-	114.8	-	50	-	12.0	-

6. SUMMARY AND CONCLUSIONS

The API RP2A-WSD, - LRFD and ISO 13819-2 code provisions for tubular members, tubular joints, grouted pile-sleeve connections and pile foundations have been examined. Differences and similarities between the codes have been identified and the statistics, where available, have been collated. The findings pertaining to each component are summarised as follows:

- Tubular Members

  All codes follow a similar philosophy in that equations are presented for members acting under each load action acting alone and then in combination. There are some differences between codes for unidirectional loading but the more significant differences are with the form of the various interaction equations. There is quite a large database for establishing the statistics and this has shown that ISO and API LRFD achieve almost identical reliabilities; a mean bias of 1.28 and COV of 0.12 would seem appropriate for future reliability studies.

- Tubular Joints

  Here again, all codes follow a similar presentation in terms of following a nominal load format. The main differences concern the interaction between brace load components, and in the formulations of the basic strength parameter Qu and chord load factor Qf. API LRFD and WSD have the same Qu and Qf formulations, but ISO differs. A full set of statistics for Qu has been presented, Table 3.3, and a more limited set with Qf (chord load factor) incorporated in Table 3.4. Recommendations for overall statistics are given in Section 3.3. These are tentative due to lack of knowledge on the full role of Qf and other aspects such as brace load interaction effects and joint classification issues.

- Pile-Sleeve Grouted Connections

  The ISO provisions for pile-sleeve grouted connections are very different from those of API. The ISO provisions have a different dependency on grout strength as well as introducing pile and sleeve geometric parameters. The statistics for the ISO provisions have been inferred from the ISO commentary and background papers, but it has not been possible to produce corresponding values for API.

- Pile Foundations

  The ISO and API provisions are almost identical, only differing in the ‘K’ parameter used in the estimation of pile capacity in cohesionless soils. It has been deduced that this leads to an increase in the ISO mean bias, by a factor of 1.07 for a typical pile design, over that of API. However, there appears to be no readily available collated database in the public domain to be able to provide absolute values of the mean biases or of COVs. This is a cause of some concern as there is sufficient evidence to show that pile capacity is characterised by large variation. Furthermore, there have been a number of recent studies which demonstrate that structural reliability is significantly affected by foundation behaviour.

REFERENCES

1.1 International Standards Organisation. "ISO 13819-2 Draft D. Petroleum and Natural Gas Industries – Offshore Structures – Part 2: Fixed Steel Structures". Committee Draft, Document Reference ISO/TC 67/SC 7 N222, May 1999.

1.2 American Petroleum Institute. "Recommended Practice for Planning, Designing and Constructing Fixed Offshore Platforms – Load and Resistance Factor Design". API RP2A LRFD, First Edition, July 1993. (Together with Errata slip issued October 1993.)

1.3 American Petroleum Institute. "Recommended Practice for Planning, Designing and Constructing Fixed Offshore Platforms – Working Stress Design". API RP2A WSD, Twentieth Edition, July 1993.

2.1 Frieze PA, Hsu TM, Loh JT and Lotsberg I. "Background to Draft ISO Provisions on Intact and Damaged Members." Behaviour of Offshore Structures (BOSS), 1997.

3.1 MSL Engineering Limited. "Assessment Criteria, Reliability and Reserve Strength of Tubular Joints." MSL Doc. Ref. C14200R018, Ascot, England, March 1996.

3.2 Dier A F and Lalani M. "New Code Formulations for Tubular Joint Static Strength." 8th International Symposium on Tubular Structures, Singapore, August 1998.

4.1 Harwood R G, Billington C J, Buitrago J, Sele A B and Sharp J V. "Grouted Pile to Sleeve Connections: Design Provisions for the New ISO Standard for Offshore Structures". Offshore Mechanics and Arctic Engineering (OMAE) Conference, Florence, June 1996.

4.2 Bomel. Attachment Item 3c to Minutes of Meeting held 30 March 2000, Doc. Ref. C894/07/022U.

4.3 Karsan D I and Krahl N W. "New API Equation for Grouted Pile-to-Structure Connections". Paper OTC 4715, Offshore Technology Conference, Houston, May 1984.

Printed and published by the Health and Safety Executive
C0.50 3/01

MAIL ORDER
HSE priced and free
publications are
available from:
HSE Books
PO Box 1999
Sudbury
Suffolk CO10 2WA
Tel: 01787 881165
Fax: 01787 313995
Website: www.hsebooks.co.uk

RETAIL
HSE priced publications
are available from
good booksellers

HEALTH AND SAFETY ENQUIRIES
HSE InfoLine
Tel: 08701 545500
or write to:
HSE Information Centre
Broad Lane
Sheffield S3 7HQ
Website: www.hse.gov.uk

OTO 2000/072

£10.00

ISBN 0-7176-1975-3